L-phenylalanine and trans-cinnamic acid combined with Fe3O4-NPs treatment induce oxidative stress and enhances alkaloid production in Narcissus tazetta L. by increasing PAL and N4OMT gene expression

LADAN BAYAT

AZRA SABOORA

EZAT ASGARANI

MAHBOOBEH ZARRABI

TÜBİTAK

L-phenylalanine and *trans*-cinnamic acid combined with Fe$_3$O$_4$-NPs treatment induce oxidative stress and enhances alkaloid production in *Narcissus tazetta* L. by increasing *PAL* and *N4OMT* gene expression

Ladan BAYAT[1], Azra SABOORA[1,*], Ezat ASGARANI[2], Mahboobeh ZARRABI[2]

[1]Department of Plant Sciences, Faculty of Biological Sciences, Alzahra University, Tehran, Iran
[2]Department of Biotechnology, Faculty of Biological Sciences, Alzahra University, Tehran, Iran

Abstract: The medicinal properties of narcissus plants are attributed to the presence of Amaryllidaceae alkaloids. Elicitors, such as nanoparticles, are employed to enhance the production of secondary metabolites through signaling and the generation of reactive oxygen species. We investigated the effects of Fe$_3$O$_4$ nanoparticles (Fe$_3$O$_4$-NPs), *trans*-cinnamic acid (*t*CA), and L-phenylalanine (L-Phe) precursors on various physiological and biochemical parameters in *Narcissus tazetta* L., with a particular focus on alkaloid content. Fe$_3$O$_4$-NPs treatment significantly increased photosynthetic pigments, secondary metabolites (including alkaloids, phenolic compounds), total soluble carbohydrates, and polysaccharides. The activities of antioxidant enzymes (SOD, CAT, POD), phenylalanine ammonia-lyase (PAL), and tyrosine ammonia-lyase (TAL) enhanced under Fe$_3$O$_4$-NPs treatment. While *t*CA treatment led to an increase in H$_2$O$_2$ level, L-Phe treatment decreased it. Both elicitors influenced the plant's metabolism, promoting primary and secondary metabolites. The augmentation of photosynthetic pigment content and antioxidant enzyme activity induced by *t*CA and L-Phe treatments appeared to improve alkaloid production. Furthermore, in silico studies using Molegro Virtual Docker (MVD) software were conducted. The third structures of PAL and N4OMT enzymes were designed by Modeler software and the ligand structures were designed using ChemDraw® (Fe$_3$O$_4$) and Atomsk (precursors) software. Docking results revealed that the Fe$_3$O$_4$-NPs and precursors interacted with the active sites of PAL and N4OMT, two enzymes involved in alkaloid biosynthesis in narcissus, exhibiting varying binding energies and impacting their activities. The Fe$_3$O$_4$/N4OMT and L-phenylalanine/PAL complexes had higher free energies of binding. Our results indicated that Fe$_3$O$_4$-NPs and precursors significantly affected the gene expressions of *PAL* and *N4OMT*. The highest levels of *PAL* (after 96 h) and *N4OMT* (after 24 h) expressions were obtained in *t*CA + Fe$_3$O$_4$-NPs and L-Phe + Fe$_3$O$_4$-NPs treatments. In summary, the application of Fe$_3$O$_4$-NPs, *t*CA, and L-Phe demonstrated the potential to activate the production of secondary metabolites, including alkaloids, by modulating the plant's metabolic pathways.

Key words: Alkaloids, elicitor, Fe$_3$O$_4$-NPs, *N. tazetta* L., *N4OMT* gene expression, PAL

1. Introduction

Narcissus belongs to the monocotyledon family Amaryllidaceae, which comprises 85 genera and 1100 species (Bastida et al., 2011). This genus has a predominantly Mediterranean distribution but can also be found in regions such as France, Africa, and Greece. *Narcissus tazetta* L., specifically, is not limited to Spain and North Africa; it also thrives in temperate parts of Asia (Hanks, 2002). The eastward distribution of *N. tazetta* suggests historical trade routes where this plant has been highly valued as an ornamental plant species. This highlights its significance in commercial horticulture (Hanks, 2002). A distinctive characteristic of *N. tazetta* is its ability to produce Amaryllidaceae alkaloids (AA) with promising medicinal potential (Desgagné-Penix,

2020). These alkaloids exhibit diverse biological activities, including the anti-Alzheimer properties of galantamine (Hotchandani et al., 2019), the antiviral and antitumor effects of lycorine (Bastida et al., 2011), and the antioxidant and anticancer properties of haemanthamine (Bastida et al., 2011; Van Goietsenoven et al., 2010). The substantial medicinal application of Amaryllidaceae alkaloids is evident in the use of galantamine to treat Alzheimer's disease, already commercialized as a drug (Evidente, 2023) under the brand name Reminyl© (galantamine hydrobromide) (Hulcová et al., 2019). Galantamine can inhibit the enzyme acetylcholinesterase (AChE), which plays a crucial role in Alzheimer's disease (Evidente, 2023).

While *Narcissus* plants contain a wealth of Amaryllidaceae alkaloids (AAs), their content is often

---

* Correspondence: saboora@alzahra.ac.ir

quite low. Additionally, the complex structures of these alkaloids make chemical synthesis challenging. Consequently, the large-scale production of AAs can be difficult and costly (Hotchandani et al., 2019). To address this challenge, alternative and cost-effective methods for increasing the yield of these valuable medicinal compounds are needed. One such approach involves the use of elicitors. The use of various elicitors has been identified as one of the most important economic and useful strategies for enhancing the production efficiency of valuable metabolites like Amaryllidaceae alkaloids in recent studies (Hadizadeh et al., 2019). Elicitation is regarded as one of the most practical biotechnological tools for inducing biosynthesis and accumulation of alkaloids (Halder et al., 2019). Elicitors, such as nanoparticles, can impact secondary metabolites like alkaloids through the production of reactive oxygen species (ROS), modulation of gene expression, and signaling pathways (Abdelkawy et al., 2023). Their interactions with cell receptors induce immediate defense responses such as improved ion flow through the plasma membrane, activation of genes involved in alkaloid biosynthesis, production of various ROS, structural changes in the cell wall, and modifications in osmotic stress (Hadizadeh et al., 2019).

Nanotechnologies have garnered significant attention due to their remarkable properties, with applications spanning various fields (Vance et al., 2015). Nanoparticles are readily absorbed by plants, effectively addressing deficiencies and enhancing growth (Harsini et al. 2014). Plants can absorb nanoparticles through different pathways, including the leaf cuticle, leaf stomata, and roots (Wang et al., 2023). The surface of cuticle layers features two distinct channels: hydrophilic and lipophilic (Avellan et al., 2019). Hydrophilic channels facilitate the diffusion of hydrophilic nanoparticles with a diameter of less than 4.8 nm. Lipophilic channels on the surface of the cuticle enable the passage of lipophilic nanoparticles, which are absorbed in leaves through diffusion and infiltration (Wang et al., 2023). Contact between the nanoparticles and the plant root occurs through root surface absorption. The formation of lateral roots can create a new adsorption interface for nanoparticles, allowing them to enter the main root (Wang et al., 2023). Upon entry into plant tissue, nanoparticles can access cells through various pathways, including ion channels, endocytosis, binding to cell membrane proteins, or physical damage (Lv et al., 2019). In the realm of plant biotechnology, the use of nanoparticles as nonbiological elicitors holds great promise for inducing the biosynthesis of secondary metabolites, including alkaloids (Rivero-Montejo et al., 2021). Among iron oxide forms, Fe_3O_4 nanoparticles (Fe_3O_4-NPs), also known as magnetite, black iron oxide, magnetic iron ore, and loadstone (Ghazanfari et al., 2016), are widely recognized and extensively used,

especially in biomedical applications (Kafayati et al., 2013). The interaction between nanoparticles and plants depends on several factors, including concentration, size, physical characteristics, and plant species. This interaction can result in biochemical, physiological, and morphological changes. For instance, soybean treated with iron oxide nanoparticles exhibited alterations in chlorophyll content and photosynthetic efficiency. Similarly, tobacco plants subjected to Fe_3O_4-NPs (5 nm diameter), displayed a reduced photosynthetic rate and leaf area but increased protein accumulation compared to control plants (Alkhatib et al., 2020). A study by Feng et al. (2022) demonstrated that high concentrations of iron oxide nanoparticles (200 and 500 mg L^{-1}) increased the growth of wheat plants.

Another strategy to enhance secondary metabolite production in plants involves the addition of specific precursors to the biosynthetic pathway of these compounds (Hussain et al., 2012). If nutrients and hormones added to the culture medium can boost secondary metabolite production, the introduction of precursors can further activate biosynthetic pathways. Phenylalanine and tyrosine are noteworthy amino acid precursors in this context. Teixeira et al. (2017) investigated changes in antioxidant enzyme activities after phenylalanine spray on soybean leaves and seeds. Their results showed that catalase (CAT), peroxidase (POD), and superoxide dismutase (SOD) activity decreased, while the activity of the phenylalanine ammonia-lyase (PAL) and lipid peroxidation value significantly increased compared to the control. The use of appropriate concentrations of nanoparticles (NPs) and precursors may increase the expression of the key genes and consequently the content of *Narcissus* alkaloids including galantamine, lycorine, and narciclasine.

Figure 1 illustrates key genes at the outset of the narcissus alkaloid biosynthesis pathway: phenylalanine ammonia-lyase (*PAL*) and norbelladine-4'-O-methyltransferase (*N4OMT*) (Hotchandani et al., 2019). PAL serves as a pivotal regulatory enzyme, converting phenylalanine to cinnamic acid and directing carbon flow from the shikimate pathway to phenylpropanoid metabolism. Consequently, PAL plays a vital role in connecting primary metabolism to secondary metabolism, leading to the production of various chemicals, including phenolic and alkaloid compounds (Desgagné-Penix, 2020). N4OMT, on the other hand, catalyzes the initial specific reaction in Amaryllidaceae alkaloid biosynthetic by methylating norblladine to 4'-O-methylnorblladine. Several sequences and transcripts of N4OMT have been identified in some species of Amaryllidaceae, including *N. pseudonarcissus*, *N. papyraceus*, *L. radiata*, *L. aurea*, and *Rhodophiala bifida* (Desgagné-Penix, 2020). This enzyme has a homodimer protein structure (Li et al., 2019).
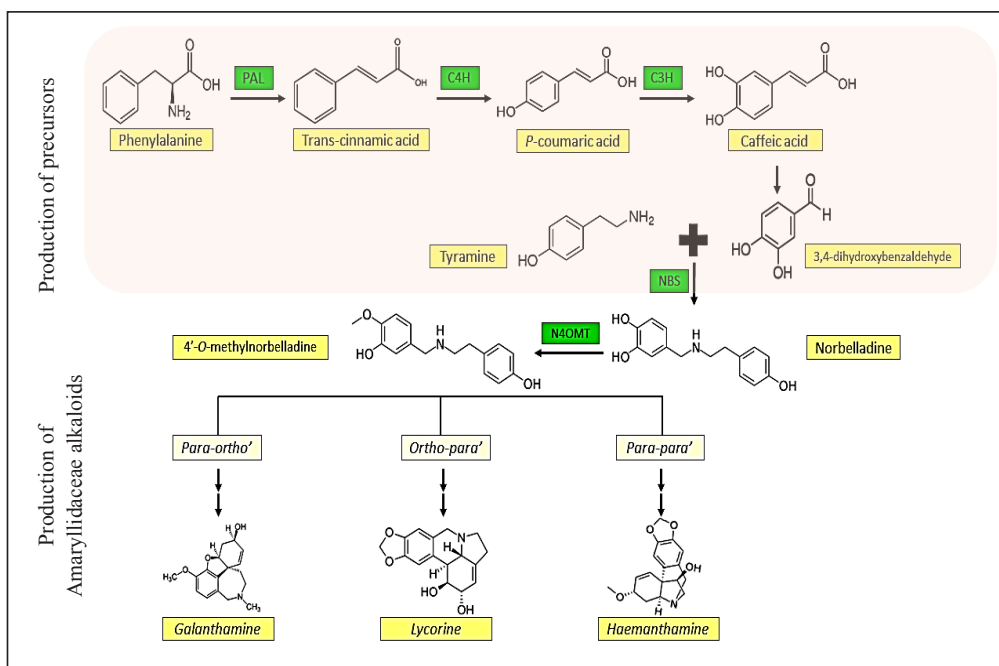
Figure 1. Production of narcissus alkaloids from phenylalanine metabolism to Amaryllidaceae alkaloids (AA) in *Narcissus* species. Abbreviations: PAL, phenylalanine ammonia lyase; C4H, cinnamate 4-hydroxylase; C3H, coumarate 3-hydroxylase; NBS, norbelladine synthase; N4OMT, norbelladine 4′-O-methyltransferase (Adopted from Hotchandani et al., 2019).

Few studies have explored the optimization of medicinal alkaloid production in *Narcissus tazetta*. In this study, we investigate the impact of Fe_3O_4-NPs and two precursors on biochemical parameters in *N. tazetta* and the gene expression of *PAL* and *N4OMT*, both crucial enzymes in the biosynthetic pathway of *Narcissus* alkaloids. To gain molecular insights and interpret the microscopic events that occurred in our experiment, we utilized in silico computational simulation as a powerful tool for assessing the interaction between nanoparticles, precursors, and biomolecules. These models, in conjunction with in vitro data, enable the prediction of chemical reactions. Computational analyses containing electronic structure methods using molecular docking were employed to obtain more insights into the interactions and dynamics of elicitors like nanoparticles within biological systems (Zhdanov, 2019). Molecular docking, a fundamental component of computer-based studies, facilitates the examination of three-dimensional structures of protein-ligand complexes. Consequently, we employ molecular docking to elucidate how precursors bind to relevant enzymes and how nanoparticles influence the activity of specific enzymes within the studied biosynthetic pathways. Molecular docking can predict interaction and binding energies between nanoparticles and macromolecules (Abdelsattar et al., 2021). Gandhi and Roy (2019) studied the interaction of bovine serum albumin (BSA) with $MnFe_2O_4$ nanoparticles to predict their binding with the bloodstream proteins, with a binding energy of 27.36 kcal/mol. In another study, the interaction of acetylcholinesterase (AChE) and butyrylcholinesterase (BChE) enzymes, important biological targets for the treatment of Alzheimer's disease, with Fe_3O_4-NPs was predicted. The binding energies were 2.31 and 1.78 kcal/mol, respectively (Khalil et al., 2018).

2. Materials and methods

2.1. Nanoparticle characterization

Fe_3O_4 nanoparticles were obtained from Mashhad Nanosadra Co., Iran, with a purity exceeding 98%. These nanoparticles had the following specifications: average particle size (APS): 20–30 nm, specific surface area (SSA): 40–60 m^2 g^{-1}, color: dark brown, morphology: spherical, bulk density: 0.84 g cm^{-3}, true density: 4.8–5.1 g cm^{-3}. Characterization of the Fe_3O_4-NPs is presented in Figure 2 through field-emission scanning electron microscope (FESEM) analysis with two zoom scales, 1 μm and 100 nm. The particles appeared to be more or less spherical with a particle size of 20–30 nm. They homogenously aggregated with well-separated grain boundaries. Additionally, *trans*-cinnamic acid and L-phenylalanine were procured from Sigma-Aldrich Co. (United States) and used for the treatments.
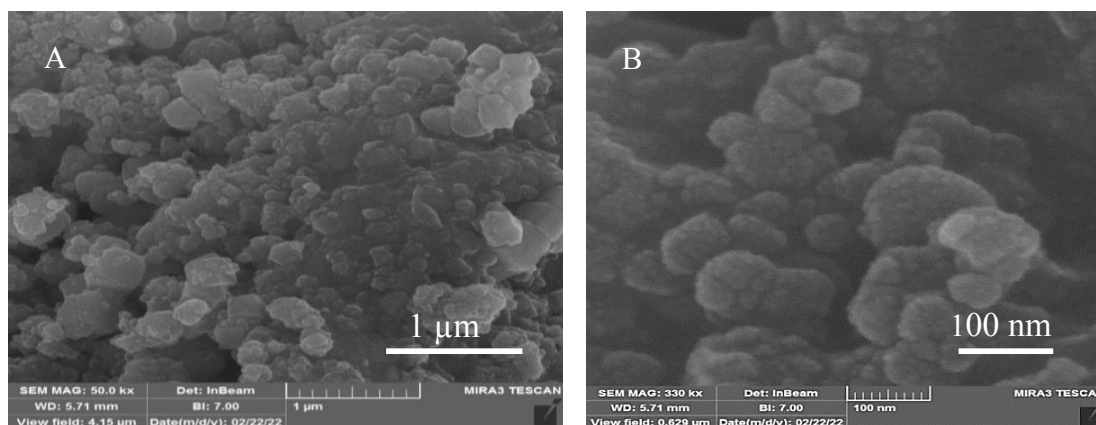
Figure 2. FESEM images of Fe_3O_4-NPs with two zoom scales, 1 μm (A) and 100 nm (B).

2.2. Plant cultivation and treatment

Bulbs of *N. tazetta* L. var. Shahla were soaked in water for 2 h and then planted at a depth of 15 cm in the research farm at Alzahra University. The photoperiod was 11 hours of light and 13 hours of darkness, with daily temperatures ranging from 21 to 26 °C during the day and 14 to 11 °C at night. The relative humidity during the growing period varied between 70% and 90%.. Rows were spaced 20 cm apart, with bulbs within each row spaced 10 cm apart. Initially, the plots received twice-weekly watering, followed by weekly irrigation. Treatment of the plants involved applying various solutions to the leaves of 3-month-old plants. These solutions included: distilled water (used as the control), 500 mg L^{-1} Fe_3O_4-NPs, 200 mg L^{-1} *trans*-cinnamic acid, 200 mg L^{-1} L-phenylalanine, and two treatments consisting of Fe_3O_4-NPs in combination with one of the aforementioned precursors. All treatments were applied as a leaf spray (one time) until the leaves were thoroughly wet. Measures were taken during treatments to prevent soil contamination by the chemicals used. Since changes in gene expression levels occur much more rapidly than changes in metabolite contents, Leaf samples were harvested for gene expression analysis 24 h and 4 days after the applied treatments. Sampling for physiological and biochemical assays was conducted on the 2nd and 15th days after applied treatments. Leaf samples were promptly frozen at –70 °C

2.3. Measurement of Fe^{3+} content in plant samples

Dry leaf powder (120 mg) was mixed with 10 mL of an acidic solution containing 10% acetic acid and 0.1 M nitric acid. The mixture was shaken at 120 rpm for 24 h, followed by centrifugation at 10,000 rpm for 20 min. The resulting supernatant was quantitatively analyzed to determine the Fe^{3+} ion concentration by the ICP-OES (Inductively Coupled Plasma Optical Emission Spectroscopy) method (Elekes et al., 2010).

2.4. Analysis of physiological and biochemical changes

2.4.1. Determination of H_2O_2 content

To evaluate hydrogen peroxide (H_2O_2) content in the leaf tissue, 0.4 g of the fresh sample was homogenized in 4 mL of 0.1% trichloroacetic acid (TCA) and centrifuged at 13,000 × g for 20 min. Subsequently, 1 mL of the supernatant was mixed with 1 mL of potassium phosphate buffer (0.1 M, pH 7) and 2 mL of potassium iodide (1 M). The absorbance of the reaction mixture was measured at 390 nm. H_2O_2 content was estimated using the method described by Velikova et al. (2000).

2.4.2. Malondialdehyde (MDA) content

Lipid peroxidation assays were employed to assess oxidative damage and antioxidant productivity. A 0.5 g fresh leaf was extracted with 2.5 mL of 0.1% trichloroacetic acid (TCA) and centrifuged at 4000 × g for 10 min. To 1 mL of the supernatant, 4 mL of 20% TCA solution containing 0.5% thiobarbituric acid (TBA) was added. The mixture was heated in a boiling water bath for 30 min and then immediately cooled in an ice bath. After centrifugation at 10,000 × g for 10 min, the absorbance of the supernatant was measured at 532 and 600 nm using spectrophotometry. This method detects the production of malondialdehyde (MDA) and its reaction with TBA, forming a colored MDA-TBA complex. The MDA content was quantified using the extinction coefficient of 155 mM^{-1} cm^{-1}, with subtraction of the nonspecific absorption at 600 nm (Heath and Packer, 1968).

2.4.3. Determination of antioxidant enzyme activities

To extract total soluble protein, 1 g of leaf sample was ground with liquid nitrogen and homogenized in 5 mL of potassium phosphate buffer (0.05 M, pH 7.2). The homogenate was centrifuged at 15,000 × g for 30 min at 4 °C, and the resulting supernatant was stored at –70 °C for the antioxidant enzyme assays. Prior to the assays, the protein concentration was determined using Bradford method (Bradford, 1976).

For the estimation of superoxide dismutase (SOD) activity, a reaction mixture was prepared by combining 100 mL of potassium phosphate buffer (0.2 M, pH 7) with 0.194 g of methionine, 0.0021 g of nitro blue tetrazolium (NBT), and 0.0028 g of riboflavin. To 1.5 mL of the reaction mixture, 50 μL of protein extract was added and the mixture was exposed to a fluorescent lamp for 18 min. The absorbance was measured at 560 nm. SOD activity was defined as the amount of enzyme that causes a fifty percent inhibition of the photochemical reduction of NBT (Beauchamp and Fridovich, 1971).

Peroxidase (POD) activity was determined following the method described by Liu et al. (1999). The enzyme's reaction mixture consisted of 0.95 mL sodium citrate buffer (0.1 M, pH 6), 1 mL of 15 mM guaiacol, and 50 μL of protein extract. The reaction was initiated by adding 1 mL of 32 mM hydrogen peroxide (H_2O_2) and absorbance was recorded at 470 nm for up to 3 min. POD activity was calculated using the extinction coefficient of guaiacol and expressed as units per milligram of protein.

The method of Dazy et al. (2008) was employed to determine catalase (CAT) activity. In this assay, a reaction mixture containing 2.5 mL of potassium phosphate buffer (0.05M, pH 7) and 0.2 mL of protein extract was prepared. The enzymatic reaction was initiated by adding 0.3 mL of 3% H_2O_2. Catalase activity was measured at 240 nm by monitoring the decomposition of H_2O_2. CAT activity was expressed as units per mg of protein.

2.4.4. Total phenolic and flavonoid content assay

To extract phenolic compounds, 0.1 g of dry leaf powder was ground and mixed with 10 mL of 70% ethanol. The mixture was shaken at 100 rpm for 24 h, followed by centrifugation at 10,000 × g for 15 min. The resulting supernatant was used for further assays.

Total phenolic content was determined colorimetrically using the Folin-Ciocalteu reagent (Tunc-Ozdemir et al., 2009). To 0.2 mL of the extract, 0.2 mL of Folin-Ciocalteu reagent (0.2 M) and 1.8 mL of distilled water were added. After 5 min, 2 mL of sodium carbonate solution (7% Na_2CO_3) was added, and the final volume was adjusted to 5 mL with distilled water. The mixture was incubated for 90 min, and the absorbance was measured at 750 nm. Total phenolic content was expressed as milligram of gallic acid equivalent per gram of dry weight.

Total flavonoid content was determined colorimetrically using aluminum chloride (Zhishen et al., 1999). To 0.2 mL of the extract, 4.5 mL of ethanol (90%), 0.2 mL of aluminum chloride (2%), and 0.1 mL of aqueous acetic acid (33%) were added and thoroughly mixed. After 30 min, the absorbance was measured at 414 nm. Total flavonoid content was expressed as milligram of quercetin equivalent per gram dry weight.

2.4.5. PAL and TAL activity assays

To prepare the enzyme extract, 0.1 g of fresh leaf was flash-frozen by exposure to liquid nitrogen, then ground and treated with 2mL of Tris-HCl buffer (pH 8.8, containing 15 mM β-mercaptoethanol) at 4 °C. The mixture was then centrifuged at 15,000 × g for 20 min at 4 °C, and the resulting supernatant was used to measure enzyme activity.

Phenylalanine ammonia-lyase (PAL) catalyzes the conversion of phenylalanine to *trans* cinnamic acid (*t*CA). In this method, L-phenylalanine was used as a substrate. PAL activity was measured by the production of *t*CA. The assay mixture contained 1 mL of Tris-HCl buffer (pH 8.8, containing 15 mM β-mercaptoethanol), 0.5 mL of 10 mM L-phenylalanine, 350 μL of double distilled water, and 150 μL of the extract. After incubation for an hour at 37 °C, the reaction was stopped by adding 0.5 mL of HCl (6 M), and the reaction product was extracted with 10 mL of ethyl acetate. The samples were evaporated under airflow, and the solid precipitate was dissolved in 3 mL of NaOH (0.05 M). The absorbance was measured at 290 nm. One unit of PAL activity was determined as the amount of enzyme that produces 1 μmol *t*CA per hour. The concentration of *t*CA was determined using the extinction coefficient of *t*CA at 290 nm which is equal to 9500 M^{-1} cm^{-1} (Kyndt et al., 2002).

Tyrosine ammonia-lyase (TAL) activity was measured similarly to the PAL assay method with a slight modification. The assay mixture contained 1 mL of Tris-HCl buffer (pH 8.8, containing 15mM β-mercaptoethanol), 0.5 mL of 5.5 mM L-tyrosine, 350 μL of double distilled water, and 150 μL of the extract. All conditions and procedures were performed as mentioned in the protocol for the PAL assay, but TAL activity was evaluated by monitoring the increase in the absorbance at 310 nm (Kyndt et al., 2002). One unit of TAL activity was defined as the amount of the enzyme that produced 1 μmol *p*-coumaric acid (*p*CA) per hour. The *p*CA concentration was determined using the extinction coefficient of this compound at 310 nm, which is equal to 1000 M^{-1} cm^{-1}.

2.4.6. Determination of total alkaloid content

The modified method of Renaudin (1984) was used to measure the total alkaloid content. One gram of dry powdered leaves was mixed with 25 mL of methanol and sonicated for 10 min in an ultrasonic bath. Subsequently, the mixture was shaken at 100 rpm for 24 h. The sonication process was repeated for 20 min, and the samples were centrifuged at 10,000 × g for 10 min. The supernatant was separated, and the precipitate was washed with 5 mL methanol. Next, the extracts were evaporated under a vacuum. The dry extract was dissolved in 4 mL of sulfuric acid (3%) and defatted with 15 mL (3 × 5) of diethyl ether in a separating funnel. Next, the pH of this phase was adjusted to 9–10 with ammonia (25%), and finally, the

alkaloid compounds were extracted with 21 mL (3 × 7) of chloroform. A small amount of anhydrous sodium sulfate was added to the chloroform solution, and after 10 min, the solution was centrifuged, and the supernatant was evaporated to dryness. Subsequently, 10 mL of absolute ethanol was added to the precipitant for the alkaloid assay. The absorbance was measured at 259 nm, and the galanthamine alkaloid was used as the standard (Klosi et al., 2016).

2.4.7. Photosynthetic pigment contents
To determine the content of photosynthetic pigments, 0.2 g of fresh leaf was ground with 80% acetone and centrifuged at 4000 × g for 5 min. Subsequently, the absorbance of the supernatant was measured using the spectrophotometer at 663, 646, and 470 nm. The contents of Chl a, Chl b, and total carotenoids were estimated based on the equation of Lichtenthaler (1987).

2.4.8. Sugar content assay
To extract carbohydrates, 0.05 g of dry powdered leaves was mixed with 0.5 mL of ethanol 80% in an Eppendorf tube and vortexed. The mixture was subsequently centrifuged at 13,000 × g for 10 min. The supernatant was discarded, and this step was repeated three times. The collected supernatants were evaporated under vacuum, yielding a dry extract that was dissolved in warm distilled water. Subsequently, 2.5 mL of 0.3 N barium hydroxide and 2.5 mL of 5% zinc sulfate were added. After centrifugation at 15,000 × g for 15 min, the supernatant volume was adjusted to 25 mL with distilled water and utilized for the soluble carbohydrates assay. The leaf residues in the Eppendorf tubes were used for the polysaccharides assay. The leaf residues were mixed with 10 mL of distilled water and heated for 10 min in a hot water bath at 100 °C. After vortexing and centrifugation at 13,000 × g, the supernatant volume was adjusted to 25 mL with distilled water and used for determining of polysaccharide content.

To quantify the soluble carbohydrate content, 1 mL of the above extract was mixed with 1 mL of Somogyi's alkaline copper reagent (Somogyi, 1952) and heated for 20 min. Subsequently, following cooling, 1 mL of Nelson's arsenomolybdate was added, and the resultant solution was diluted with distilled water to a final volume of 12.5 mL. Finally, the absorbance was measured at 500 nm, and the soluble carbohydrates content was calculated as a percentage of the dry weight.

Measurement of polysaccharide content was conducted using the phenol-sulfuric acid method (Dubois et al., 1956). Initially, 0.5 mL of the polysaccharide extract was mixed with 1 mL of phenol (5%) and 1.5 mL of distilled water. After vortexing the mixture, 5 mL of concentrated sulfuric acid was gently added, and the mixture was incubated at room temperature for 30 min. The absorbance of the mixture was measured at 485 nm, with various concentrations of glucose employed as the standard.

2.4.9. Gene expression analysis
Total RNA was extracted from 100 mg of *N. tazetta* leaves using the Plant RNA Mini-Preps Kit (BS82314-50Preps, EZ-10 Spin Column Plant RNA Mini-Preps Kit, Bio BASIC, Canada) according to the kit supplier's recommendations. The isolated RNA was dissolved in ethanol and stored at –80 °C. The concentration of the RNA samples was determined using the ThermoFisher Scientific NanoDrop 2000 spectrophotometer, and RNA integrity was confirmed using 1% agarose gel. Subsequently, 5 µg of total RNA was used for cDNA synthesis with a reverse transcription kit (SMOBIO, Taiwan) following the manufacturer's guidelines.

The mRNA sequences of the *PAL* (GU574806.1), *N4OMT* (MH379633.1), and *Actin* (JX310699.1) genes were retrieved from the NCBI database, and the corresponding primers for amplification were designed using Oligo7 software. The *Actin* primer was chosen as a housekeeping gene (Table 1). Housekeeping genes are characterized by their stable expression across all cell types and conditions, their essential role in cellular maintenance pathways, and their conservation (Joshi et al., 2022). Several studies, including those by Chen et al. (2019) and Feng et al. (2019), have identified *Actin* as the most suitable and recommended reference gene for expression studies under abiotic stress conditions. Therefore, the *Actin* gene was selected as the housekeeping gene for this research. The efficiency of the primers was assessed by slope-based method and analyzed with LinRegPCR software for each primer. The summarized results are presented in Table 1.

Table 1. Specificity of the primers designed for *PAL1*, *N4OMT*, and *Actin* genes.

Gene	Direction	Primer sequence (5' to 3')	Length (bp)	Primer efficiency
PAL1	Forward	AAGTCGAAAACGCCAGGGTA	20	1.86
	Reverse	AACATTCTCGCCCGTAAGCA	20	
N4OMT	Forward	CGACGACTACTGCCTCATCC	20	1.83
	Reverse	CTTCTCGGTCACCTCCCTGA	20	
Actin	Forward	GTGTTGGATTCTGGTGATGG	20	1.87
	Reverse	GGACAATTTCACGCTCAGCA	20	

A real-time polymerase chain reaction (RT-qPCR) was performed utilizing the StepOn real-time PCR system (ThermoFisher Scientific, USA) using SYBR Green as the intercalating dye. The expression levels of the target genes were quantified and normalized relative to an endogenous reference and a calibrator using $2^{-\Delta\Delta CT}$ method (Livak and Schimittgen, 2001). Nucleotide sequence alignments and comparisons were conducted using the Basic Local Alignment Search Tool (BLAST) program[1].

The gene sequencing of RT-qPCR products was conducted to confirm their identity as the selected genes. The RT-qPCR products of the genes were sent to Pishgam Biotechnology Co. (Iran) for sequencing. Subsequently, sequencing results were consolidated by Bioedit software, followed by gene alignment with reference sequences obtained from NCBI.

2.4.10. In silico study

To investigate the impact of Fe_3O_4-NPs on specific enzymes involved in the alkaloids biosynthesis pathway of *N. tazetta*, the gene sequences of PAL1 and N4OMT enzymes were initially aligned separately using the NCBI blast tool[2]. For PAL1, the nucleotide sequence related to the *Narcissus tazetta* (GU574806.1) was retrieved from the nucleotide section of the NCBI website in FASTA format and then subjected to BLAST analysis. However, in the case of N4OMT, since the gene sequence was not available, the sequence was reverse-translated from protein to gene using the EMBL-EBL program[3], based on the protein sequence (AXL96676.1) of N4OMT (norbelladine 4'-O-methyltransferase) from *N. tazetta* obtained from the protein section of the NCBI website. The protein sequence was copied in FASTA format. This sequence was translated into nucleotide sequence program[4]. The corresponding nucleotide sequence was blasted in the Nucleotide BLAST section of the NCBI site. Subsequently, the tertiary structure of each enzyme was generated using the Modeler program, followed by energy minimization (structures optimization) using the 3Drefine online software[5]. The ligand structure of Fe_3O_4-NPs was designed using ChemDraw online software[6]. Finally, molecular docking simulations were performed utilizing the Molegro Virtual Docker 5.5 software.

2.4.11. Statistical analysis

All experiments were performed with a minimum of three independent replicates in a completely randomized design. The results of biochemical and physiological analysis of the plant samples treated with Fe_3O_4-NPs and the studied precursors were presented as means ± standard error (SE). Data were statistically analyzed using SPSS software (version 26, SPSS Inc., IL, USA). Differences between treatments were assessed using one-way analysis of variance (ANOVA), with significant differences between the treatment group and control denoted at p ≤ 0.05 as determined by Duncan's test. Subsequently, principal component analysis (PCA) was used to transform the data into lower dimensions. Variables with the greatest impact and strong correlations were identified using SRplot (Science and Research online plot)[7].

3. Results

To confirm the penetration of nanoparticles into plant tissue treated with Fe_3O_4-NPs, we examined the concentration of Fe^{+3} element in leaf tissues using the ICP-OES method. The results showed a significant increase in the treated tissue compared to the control (Table 2). Subsequently, we carried out additional experiments, the results of which are presented below.

3.1. Changes in H_2O_2 and MDA contents

Treatment with nanoparticles often leads to the generation of reactive oxygen species (ROS). However, the measurement of H_2O_2 levels indicated a significant decrease in H_2O_2 content in leaf tissues of *N. tazetta* L. treated with 500 mg Fe_3O_4-NPs compared to the control (Figure 3A). Application of *t*CA precursor resulted in a significant increase in H_2O_2 levels, especially evident after 15 days of treatment (0.23 μmol g^{-1} FW against 0.17 μmol g^{-1} FW). This represented the most substantial increase, approximately 1.35 times higher than the control, observed in this treatment. Conversely, the application of L-phenylalanine led to a reduction in H_2O_2 content relative to the control (0.11 μmol g^{-1} FW against 0.17 μmol g^{-1} FW). As shown in Figure 3A, the combined treatment of Fe_3O_4-NPs with each precursor further decreased H_2O_2 content, reaching 0.1 and 0.05 μmol g^{-1} FW against 0.17 μmol g^{-1} FW (33% and 67% lower than the control) with L-Phe+ Fe_3O_4-NPs treatment on the 2nd and 15th days, respectively. Additionally, after *t*CA+ Fe_3O_4-NPs treatment, H_2O_2 content reduced to the control level on the 2nd and 15th days (Figure 3A).

[1] http://www.ncbi.nlm.nih.gov/blast/

[2] https://blast.ncbi.nlm.nih.gov/Blast.cg

[3] https://www.ebi.ac.uk

[4] https://www.ebi.ac.uk/Tools/st/emboss_backtranseq

[5] http://sysbio.rnet.missouri.edu/3Drefine/

[6] https://chemdrawdirect.perkinelmer.cloud/js/sample/index.html
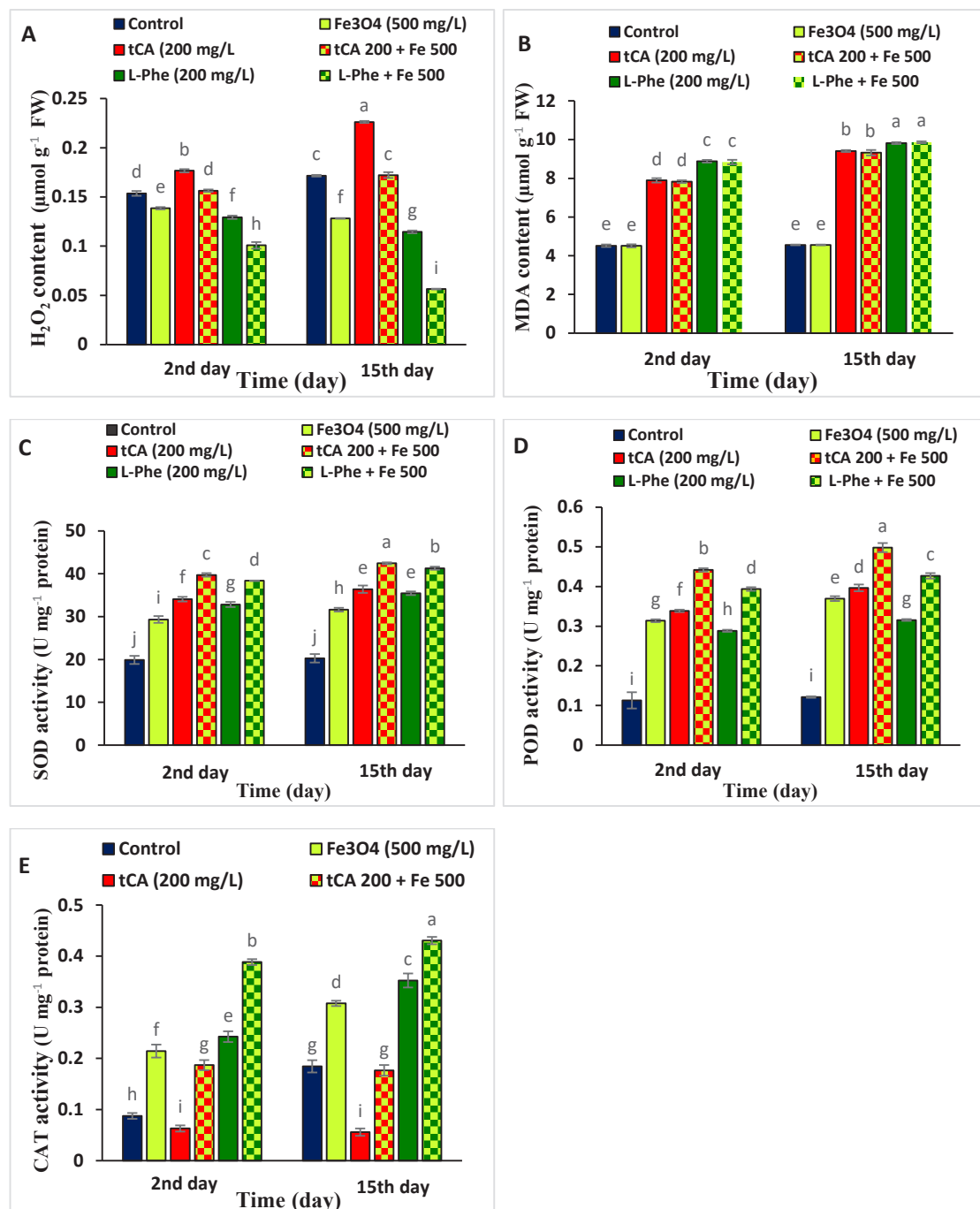
[7] https://www.bioinformatics.com.cn/en

Table 2. Concentrations of Fe^{+3} element in the leaf samples of the *N. tazetta* plant by ICP-OES method.

Plant sample	Fe^{+3} concentration (ppm)
Control	0.69
Treated with Fe_3O_4-NPs	1.61

Figure 3. Comparison of mean H_2O_2 and MDA contents (A, B), and changes in enzyme activity of the SOD, POD, and CAT (C, D, E) in the leaves of *Narcissus tazetta* L. following treatment with Fe_3O_4-NPs, *t*CA, and L-Phe on the 2nd and 15th days after elicitation. Different letters on the columns in each graph indicate significant differences at p ≤ 0.05, as determined by Duncan's test.

Moreover, there was no significant difference between MDA content of the leaf tissue treated with Fe_3O_4-NPs compared to the control plants on the 2nd and 15th days after treatment (Figure 3B). However, MDA content in the *N. tazetta* leaves exhibited a significant increase under precursor treatments on the 2nd and 15th days. For example, *t*CA and L-Phe treatments resulted in MDA content that was 1.75- and 1.95-fold higher than the control, respectively, on the 2nd days of the treatments (7.89 and 8.88 µmol g^{-1} FW against 4.51 µmol g^{-1} FW). Interestingly, the MDA content in leaves following the combined treatment of *t*CA + Fe_3O_4-NPs and L-Phe+ Fe_3O_4-NPs did not differ significantly from the treatments with each precursor alone. The most substantial increase in MDA content (more than 2 times relative to the control) was observed with *t*CA and L-Phe treatments alone and in combination with Fe_3O_4-NPs on the 15th day after elicitation (Figure 3B).

3.2. Changes in antioxidant enzyme activity
Comparative analysis of changes in the activity of the antioxidant enzymes in *N. tazetta* leaves under Fe_3O_4-NPs and precursor treatments, both individually and in combination, is depicted in Figures 3C and 3D. Significant differences were observed in the activity of these enzymes between treated and untreated narcissus leaves. On the 2nd day after treatments, the activities of SOD, POD, and CAT were increased by 47.53%, 181.8%, and 162.5%, respectively, compared to the control, with Fe_3O_4-NPs treatment. All precursors significantly enhanced the activities of the SOD, POD, and CAT on the 2nd and 15th days after treatments, except for CAT activity, which decreased with *t*CA treatment (0.055 U mg^{-1} protein compared to 0.18 U mg^{-1} protein in the control, representing a 69.44% decrease). However, this reduction was mitigated by the addition of Fe_3O_4-NPs to the treatment, resulting in a CAT activity of 0.19 U mg^{-1} protein with *t*CA+Fe_3O_4-NPs treatment (5.55% increase) (Figure 3E). The highest mean CAT activities were attained after L-Phe+ Fe_3O_4-NPs treatments, reaching approximately 0.39 and 0.43 U mg^{-1} protein, representing an increase of 111% and 138% on the 2nd and 15th days after treatment, respectively.

Although treatments with *t*CA and L-Phe alone proved to be effective stimuli for increasing the SOD and POD activity in *N. tazetta* leaves, the addition of iron nanoparticles intensified the effect of these two elicitors on the 2nd and 15th days after treatments. With combined treatments, there was approximately a 2-fold increase in SOD activity, a 3.5- to 4-fold increase in POD activity, and a 2.5- to 4.45-fold increase in CAT activity compared to the average activity of the corresponding antioxidant enzymes in the control (Figures 3C–3E).

3.3. Changes in contents of photosynthetic pigments, soluble sugars, and polysaccharides
Our findings demonstrate that all applied treatments led to an increase in the content of photosynthetic pigments, including chlorophyll *a*, chlorophyll *b*, total chlorophyll, and carotenoids, with the exception of *t*CA treatment, which caused a decrease in pigment contents (Figures 4A–4D). Although the changes in the content of each photosynthetic pigment between the 2nd and 15th days after treatment were not significant, the different treatments had a significant impact on changing the content of chlorophylls and carotenoids at both time points of leaf sampling.

The most substantial increase in the photosynthetic pigment contents was observed after the L-Phe + Fe_3O_4-NPs treatment. For example, with this treatment, the means of chlorophyll *a* content varied from about 7 mg g^{-1} FW to 9.28 and 9.80 mg g^{-1} FW on the 2nd and 15th days, the mean chlorophyll *b* content varied from about 4 mg g^{-1} FW to 5.67 and 6.21 mg g^{-1} FW on the 2nd and 15th days, and the mean carotenoid content varied from about 1.2 mg g^{-1} FW to 1.63 and 1.73 mg g^{-1} FW on the 2nd and 15th days. Treatment of narcissus leaves with Fe_3O_4-NPs alone or in combination with *t*CA and L-Phe elicitors caused a significant increase in the photosynthetic pigment contents, especially chlorophyll *a* and *b* (Figures 4A–4D). Conversely, treatment of narcissus leaves with *t*CA had a negative effect on the biosynthesis of chlorophylls and carotenoids or increased the decomposition of these pigments. This effect intensified over time, with the content of chlorophyll *a* decreasing from 6.42 to 5.74, chlorophyll *b* from 3.39 to 2.95, and carotenoid from 1.19 to 1.12 during the 2nd to 15th days of treatment.

As illustrated in Figures 4E and 4F, the polysaccharides and soluble sugar contents of narcissus leaves were influenced by Fe_3O_4-NPs, *t*CA, and L-phe treatments. The mean polysaccharide contents varied from about 20 mg g^{-1} DW in the control plant to 24.10–25.63 mg g^{-1} DW on the 2nd day and 32.39–33.92 mg g^{-1} DW on the 15th day after these treatments.

Similarly, soluble sugar content varied from about 34.5 mg g^{-1} FW to 41.38–45.13 mg g^{-1} DW on the 2nd day and 59.72–63.37 mg g^{-1} DW on the 15th day after treatments. Notably, these compounds increased significantly under the combined treatment of iron oxide nanoparticles and precursors, with the increase in polysaccharides and soluble sugar contents being higher on the 15th day compared to the 2nd day after treatment. The highest contents of polysaccharides and soluble sugars were obtained after the L-Phe + Fe_3O_4-NPs treatment on the 15th day, showing 1.87 and 2.13 times increase compared to the control, respectively (Figures 4E and 4F).
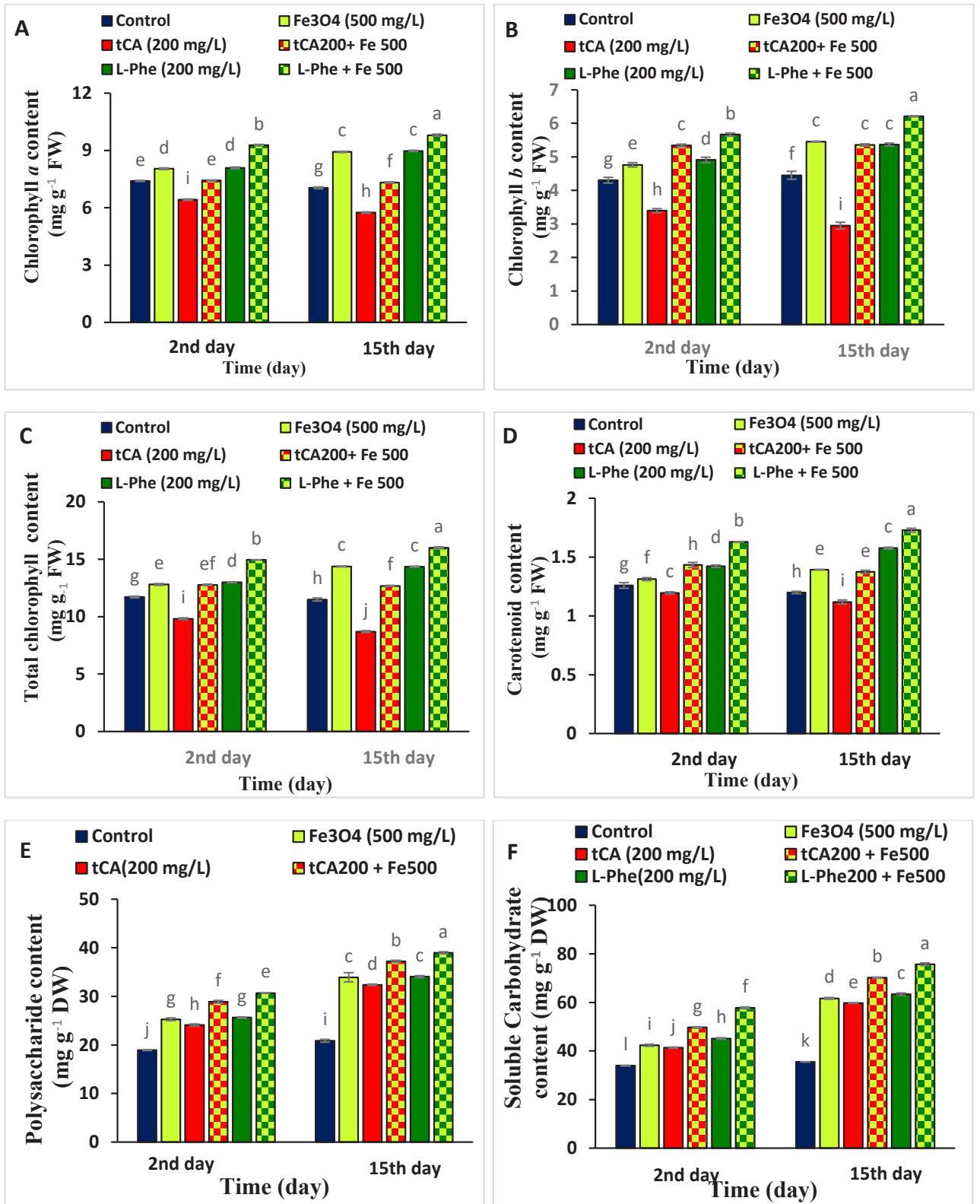
Figure 4. Comparison of mean contents of chlorophyll *a*, chlorophyll *b*, total chlorophyll, and carotenoid (A, B, C, D), and polysaccharides and soluble carbohydrates contents (E, F) in the leaves of *Narcissus tazetta* L. treated with Fe_3O_4 NPs, *t*CA, and L-Phe on the 2nd and 15th days after elicitation. Different letters on the columns in each graph indicate significant differences at p ≤ 0.05 according to Duncan's test.

3.4. Changes in phenolic, flavonoid, and alkaloid contents

As shown in Figure 5, the content of the total phenolic and flavonoid compounds in *N. tazetta* leaves significantly increased during treatment, especially with combined treatment (*t*CA+ Fe_3O_4-NPs and L-Phe+ Fe_3O_4-NPs), which exhibited the most substantial effect on the increase of these compounds on the 2nd and 15th days after elicitation. The lowest amount of the phenolic compound was measured in the control plant, ranging from 2.25 mg g^{-1} FW on the 2nd day to 2.44 mg g^{-1} FW on the 15th day. Conversely, the highest amount of this compound was estimated at 6 mg g^{-1} FW in leaves treated with *t*CA+ Fe_3O_4-NPs and L-Phe+ Fe_3O_4-NPs on the 15th day (2.5 times that of the control). After treatment with Fe_3O_4-NP, *t*CA, and L-Phe, the means of phenolic contents elevated from 2.8–3.3 mg g^{-1} FW (1.25–1.46 times that of the control) on the 2nd day to 4.25–4.67 mg g^{-1} FW (1.74–1.89 times that of the control) on the 15th day. Based on the combined treatments, phenolic contents increased from 2.08–2.11 times that of the control on the 2nd day to 2.46–2.48 times on the 15th day compared to the control (Figure 5A).

Two days after treatments, all elicitors had a similar effect on the increasing narcissus flavonoid content, reaching approximately 1.37 mg g^{-1} FW (1.8 times that of the control) in individual elicitor applications.

This compound increased to about 1.54–1.59 mg g^{-1} FW in narcissus leaves upon combined treatments, i.e. approximately 2.1 times that of the control due to the effect of *t*CA + Fe_3O_4-NPs and L-Phe+ Fe_3O_4-NPs (Figure 5B). Flavonoid levels in the narcissus leaves increased further under *t*CA, L-phe, and Fe_3O_4-NPs treatments compared to the control on the 15th day after treatments (1.78–1.84 mg g^{-1} FW against 0.83 mg g^{-1} FW). At this time, flavonoid content in narcissus leaves elevated to 2.14–2.21 times that of the control by application of Fe_3O_4-NPs and the precursors (Figure 5B). The addition of Fe_3O_4-NPs to precursor solutions intensified their effect. For example, the flavonoid content increased from a means of 1.78 mg g^{-1} FW in the leaf treated with L-Phe to a means of 2.47 mg g^{-1} FW in the leaves treated with L-Phe+Fe_3O_4-NPs (2.97 times that of the control).

Treatments of the *N. tazetta* with Fe3O4-NPs and the precursors (tCA and L-Phe) significantly increased total alkaloids in the leaf tissue. Changes in alkaloid content of the leaves were slightly higher upon combined treatments than in the mentioned individual treatments. Two days after treatment with tCA+Fe3O4-NPs and L-Phe+Fe3O4-NPs, the alkaloid contents increased about 1.66 times compared to the control (about 7.3 mg g^{-1} FW against 4.38 mg g^{-1} FW); and with Fe3O4-NPs and L-Phe treatments,
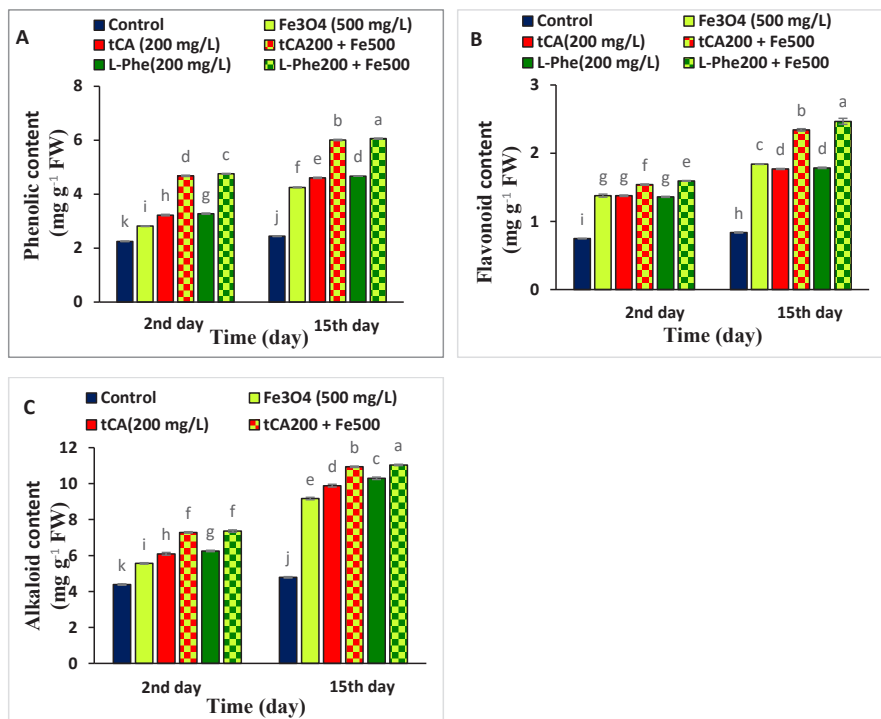
Figure 5. Comparison of mean contents of phenolics, flavonoids, and alkaloids (A, B, C) in the leaves of *Narcissus tazetta* L. treated with Fe_3O_4 -NPs, *t*CA, and L-Phe on the 2nd and 15th days after elicitation. Different letters on the columns in each graph indicate significant differences at p ≤ 0.05 according to Duncan's test.

the increase of alkaloids was 1.26 and 1.41 times more than the control, respectively. With the passage of time, 15 days after the elicitations, the content of alkaloids in the treated narcissus leaves significantly increased compared to the control. For example, alkaloid content was estimated at 9.17 mg g⁻¹ FW with Fe3O4-NPs treatment (1.92 times that of the control) and 10.93–11.03 mg g⁻¹ FW with combined treatments (2.28–2.31 times that of the control). Meanwhile, the change in the alkaloid content of the control plant was subtle during elicitation, increasing from 4.39 to 4.79 mg g⁻¹ FW (Figure 5C).

3.5. Changes in PAL and TAL activities
Our results indicated a significant increase in PAL and TAL activities in the leaves of treated plants compared to the control (Figures 6A and 6B). PAL enzyme activity in narcissus leaves showed a slight increase upon treatment with Fe_3O_4-NPs (1.4-fold of the control). However, the highest enzyme activity was observed after treatment with L-Phe + Fe_3O_4-NPs on both the 2nd and 15th days, reaching approximately three times that of the control. Additionally, the effect of L-Phe precursor alone enhanced PAL activity in leaf tissue more than the tCA treatment, with 2.7-fold and 1.7-fold increases compared to the control, respectively. Similarly, combined treatment with Fe_3O_4-NPs and tCA elicitor increased PAL activity on both the 2nd and 15th days after treatment. The increase in PAL activity exhibited a consistent pattern at both time points.

TAL enzyme activity did not show significant changes upon Fe_3O_4-NPs treatment (Figure 6B). However, two elicitors, tCA and L-Phe, whether applied alone or in combination with Fe_3O_4-NPs, markedly increased TAL enzyme activity in the leaves (Figure 6B). The highest TAL activity was recorded in narcissus leaves treated with tCA+ Fe_3O_4-NPs on both the 2nd and 15th days after

treatment, reaching 2.73-fold and 2.99-fold of the control, respectively. Similarly, the activity of the TAL enzyme significantly increased with L-Phe+ Fe_3O_4-NPs treatment, reaching 2.67-fold and 2.86-fold of the control on the 2nd and 15th days after treatment, respectively. Notably, the effect of tCA and L-Phe elicitors, when applied alone, decreased on the 15th day compared to the 2nd day of treatments.

3.6. Changes in gene expression of *PAL* and *N4OMT*
The expression of the two genes of *PAL* and *N4OMT* was analyzed in the narcissus leaves 24 and 96 h after elicitation with Fe_3O_4-NPs and precursors of tCA and L-Phe. The results are presented in Figures 7B–7D. *Actin* (housekeeping gene) exhibited constant expression in all treated tissues (Figure 7E). A significant increase in *PAL* expression was observed on the 2nd day after treatments, with fold changes ranging from 2.14 to 2.64 compared to the control. After 96 h, the highest level of the PAL gene expression was recorded in the leaves treated with tCA + Fe_3O_4-NPs and L-Phe + Fe_3O_4-NPs, showing fold changes of 5.85 and 5.95 compared to the control. Meanwhile, *PAL* gene expression increased in plants treated with Fe_3O_4-NPs, tCA, and L-Phe, with fold changes of 3.05, 3.87, and 4.49 compared to the control, respectively, albeit lower than the combined treatments (Figure 7C).

In contrast to the *PAL* gene, the expression of the *N4OMT* gene was induced much more effectively by tCA + Fe_3O_4-NP and L-Phe + Fe_3O_4-NPs treatments after 24 h, resulting in fold changes of 5.89 and 6.23 compared to the control. Application of the other elicitors alone also increased the expression of this gene by 3.63- to 4.48-fold of the control value after 24 h of treatments (Figure 7D). However, the expression of this gene decreased 96 h after elicitation (Figure 7E) under all the treatments, ranging from 1.6- to 2.28-fold compared to the control. Heatmaps of *PAL* and *N4OMT* genes displayed the relative
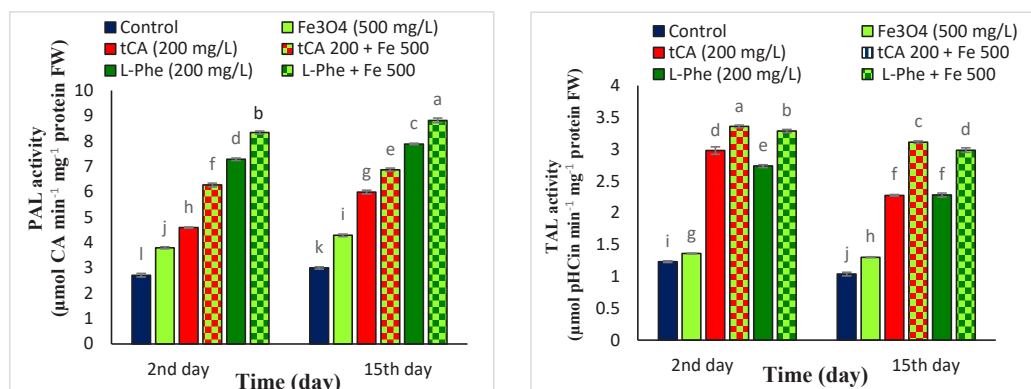
Figure 6. Comparison of mean PAL (A) and TAL (B) activities in the leaves of *N. tazetta* L. treated with Fe_3O_4 NPs, tCA, and L-Phe on the 2nd and 15th days after elicitation. Different letters on the columns in each graph indicate significant differences at p ≤ 0.05 according to Duncan's test.
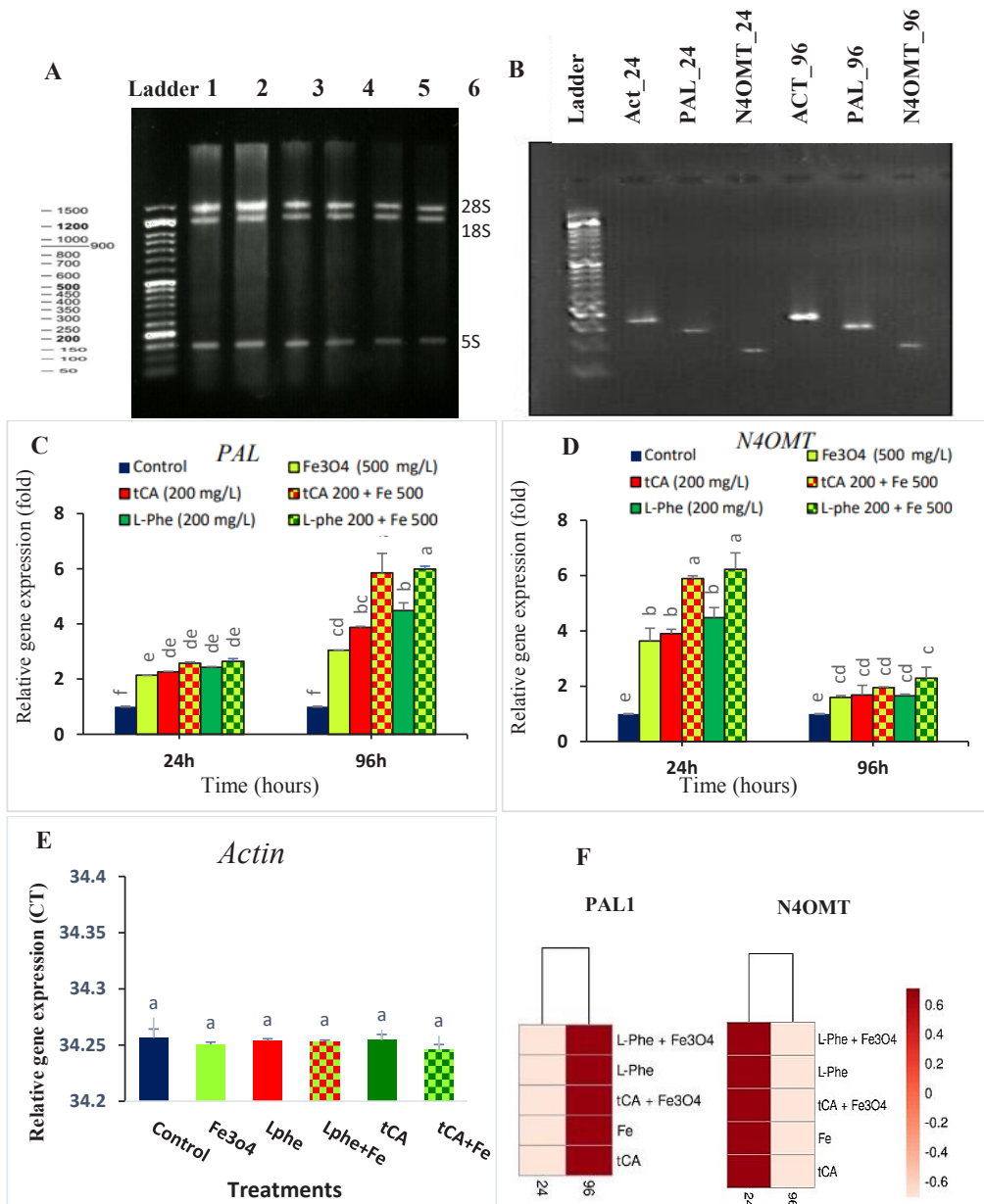
Figure 7. (A) Agarose gel electrophoresis of total RNAs from *N. tazetta* leaf tissues isolated using BIO BASIC kit. Lanes 1–6 represent RNA extracted from the control plant and the plants treated with Fe_3O_4-NPs, *t*CA, L-Phe, *t*CA+ Fe_3O_4-NPs, and L-Phe+ Fe_3O_4-NPs, respectively, after 24 h of elicitation. The bands labeled 28S, 18S, and 5S correspond to ribosomal RNA. A molecular weight indicator (Ladder) ranging from 50 bp to 1500 base pair is included. (B): Agarose gel electrophoresis of RT-PCR products of cDNA for the primers of the following genes: *ACT, PAL, N4OMT* in *N. tazetta* (lanes 1–3 on 24 h and lanes 3–6 on 96 h after treatments with Fe_3O_4-NPs and precursors). (C, D, E): Relative gene expression of *PAL, N4OMT*, and *ACT* as the housekeeping gene at 24 and 96 h after treatment. (F): Heatmaps illustrating changes in gene expressions of *PAL* and *N4OMT* in different treatments after 24 and 96 h.

expression of each gene in leaf tissue of narcissus 24 and 96 h after treatments (Figure 7F). The results of RT-qPCR products sequencing showed an acceptable query cover and identity with the mRNA sequence of *PAL, N4OMT*, and *Actin* genes in the *N. tazetta* plant (Figure 8).

The docking results revealed that Fe_3O_4-NPs and precursors effectively occupied the active sites of PAL and N4OMT enzymes and interacted with several amino acids via hydrogen bonds and steric interactions (Figures 9 and 10, Table 3). Specifically, the results of

Figure 8. PCR product sequencing and gene alignment results to confirm that the replicated sequences were our desired sequences. (A): JX310699.1 was the NCBI reference sequence of *N. tazetta* actin 2 mRNA, complete cds. (B): GU574806.1 was the NCBI reference sequence of *N. tazetta* phenylalanine MMONI-lyase (PAL1) mRNA, partial cds. C. MH379633.1 was the NCBI reference sequence of *N. tazetta* norbelladine 4-O-methyltransferase mRNA, complete cds.
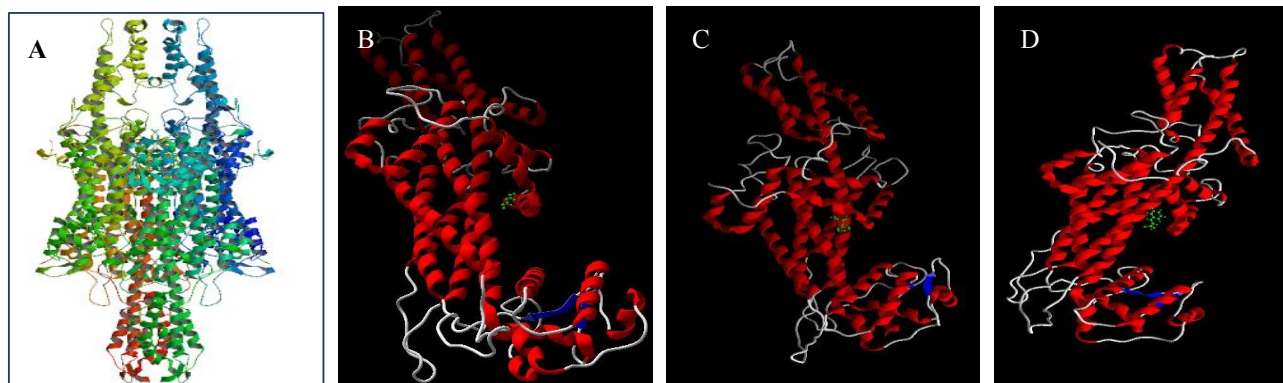
Figure 9. (A): 3D structure of PAL designed by Modeler software. (B): Molecular docking of iron oxide nanoparticle (Fe_3O_4), (C): *t*CA, and (D): L-Phe (molecule shown in green) in the active site of the PAL.

this analysis revealed the capacity of Fe_3O_4-NP to bind to the active site of PAL and N4OMT enzymes (Figures 9B and 10B), thereby influencing their activity. Further investigations demonstrated that this nanoparticle exhibited a stronger binding energy (–61.02 kcal mol^{-1}) for the N4OMT (Table 3). In contrast, in the case of the PAL enzyme, the binding energy of nanoparticles was reported as -37.38 kcal mol^{-1} (Table 3). Turning our attention to the precursors, the L-phenylalanine/ PAL complex displayed a higher free energy of binding

(–44.48 kcal mol^{-1}) compared to the L-phenylalanine/ N4OMT complex (–20.47) (Table 3). Interestingly, *t*CA exhibited a high free energy of binding for PAL (–38.7 kcal mol^{-1}) (Table 3).

4. Discussion
Elicitors have emerged as effective tools for enhancing the production of desirable secondary metabolites within the plant system (Ramachandra and Srinivasa, 2008). These compounds have the ability to activate novel genes
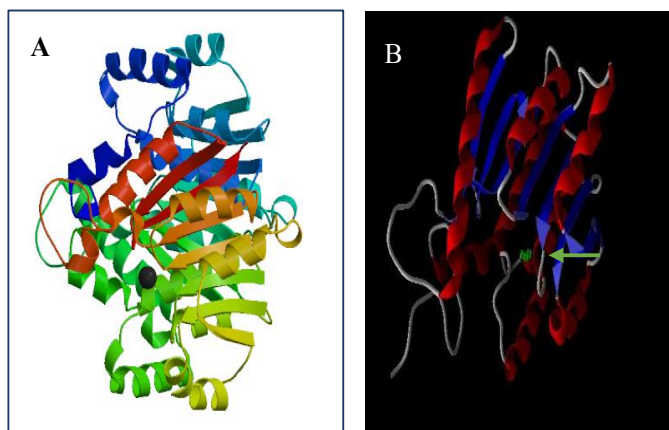
Figure 10. (A): 3D structure of N4OMT designed by Modeler software. (B): Molecular docking of iron oxide nanoparticle (Fe$_3$O$_4$ shown in green) in the active site of the N4OMT.

Table 3. Binding energy and interactions between iron oxide nanoparticles and amino acids of the studied enzymes' active site.

Enzyme	Ligand	MolDock Score	Rerank score (kcal mol^{-1})	Interaction site	
				Hydrogen bonds	Steric interaction
PAL	Fe$_3$O$_4$	1973.09	−37.38	+ Val 568 Leu 567 Ile 562	+ Leu 567 Val 568 Ile 562
	C$_9$H$_{11}$NO$_2$	-60.2893	−44.4819	-	+ Gly 565 Val 568 Leu 567 Ile 148 Ile 562 Lys 379 Leu 149
	C$_9$H$_8$O$_2$	−57.4406	−38.1707	-	+ Ile 562 Leu 567 Val 568 Ile 148 Leu 149
N4OMT	Fe$_3$O$_4$	1942.43	−61.02	+ Ser 85 Tyr 84 Val 80	+ Leu 54 Tyr 84 Ser 85 Val 80 Val 55 Tyr 239 Ser 81

C$_9$H$_{11}$NO$_2$= L-phenylalanine, C$_9$H$_8$O$_2$= *trans*-cinnamic acid; Ala= alanine, Gly= glycine, Ile= isoleucine, Leu= leucine, Lys= lysine, Ser= serine, Tyr= tyrosine, Val= valine.

and enzymes, thereby influencing various biosynthetic pathways and facilitating the synthesis of secondary metabolites (Howlett, 2006). The initiation of defense responses in plants induces a signal transduction network, typically initiated by the recognition of elicitors by cell surface receptors (Zhang et al., 2012).

In this research, three elicitors were used to improve the production of effective compounds in *N. tazetta.* Phenylalanine, an aromatic amino acid, serves as a precursor for a wide range of secondary metabolites, including phenolic acids, flavonoids, alkaloids, anthocyanins, and lignin (Feduraev et al., 2020). Its crucial role extends to various biosynthetic pathways, especially in the biosynthesis of proteins, phenolic compounds, and osmolytes which have a substantial effect on plant stress responses through signaling processes (Moe, 2013). Cinnamic acid, as the initial compound in the phenylpropanoid pathway, serves as the precursor for numerous hydroxycinnamic acid derivates and plays a key role in the synthesis of more complex phenolic compounds (Swanson, 2003). Iron (Fe) is a vital element for plant nutrition and is involved in various metabolic processes (Hu et al., 2017). It plays a fundamental role in the growth and development of plants, regulating multiple cellular processes, such as chlorophyll biosynthesis, chloroplast development, photosynthesis, respiration, RNA synthesis, and the activation of some enzymes in the biosynthesis of secondary metabolites (Feng et al., 2022; Kołton et al., 2022). Despite its abundance in the Earth's crust, the insolubility of Fe^{+3} in soils leads to iron deficiency, making it an essential nutrient.

In our study, Fe_3O_4-NPs combined with L-Phe and *t*CA induced oxidative stress, subsequently activating defense responses. This was evidenced by the increased contents of the phenolic compounds, flavonoids, and alkaloids in the leaves under the treatments. Similarly, the contents of the photosynthetic pigments and the activities of SOD, POD, and CAT were elevated. The results of principal component analysis (PCA) and Pearson's correlation analysis revealed consistent patterns of correlations between physiological variables on the 2nd and 15th days after the treatments. As shown in Figures 11A and 11B, the treatments altered the levels of variables compared to the control, with a strong positive correlation between variables (99% cumulative variance by PC1). Across both sampling times, the variables including enzymatic and nonenzymatic antioxidants were positively correlated and displayed similar distributions between the two principal components in the PC1/PC2 axes. However, certain variables such as chlorophylls, H_2O_2, and MDA showed a negative correlation with the other parameters (Figures 11C and 11D). The characters in two main categories showed divergence with the H_2O_2 parameter. A Pearson's correlation matrix was used to assess the variables, followed by clustering of the physiological and biochemical data through heatmap analysis on the 2nd and 15th days after treatment with different elicitors. The results confirmed that changes in data series displayed a strong negative correlation between H_2O_2 content and other traits (Figures 11E and 11F).

Hydrogen peroxide (H_2O_2) is a byproduct of various cellular processes, including electron transport in mitochondria and chloroplasts, as well as enzymatic reactions involving peroxisomal oxidases, NADPH oxidases, type III peroxidases, and superoxide dismutase (Smirnoff and Arnaud, 2019). In addition, H_2O_2 serves as a signal molecule under different abiotic stresses and contributes to oxidative stress response. During oxidative stress, free radicals can act as secondary messengers, triggering the accumulation of compounds such as phenolic, flavonoid, and alkaloid compounds in damaged cells and tissues. Phenolic compounds, in particular, play a critical role in scavenging reactive oxygen species (ROS) (Nourozi et al., 2019). L-Phe and *t*CA serve as initial precursors for the biosynthesis of phenolic compounds, flavonoids, and alkaloids. Their addition promotes the progression of these biosynthetic pathways, resulting in increased production of these metabolites. Our findings indicate that treatment involving Fe_3O_4-NPs and L-Phe led to decrease in H_2O_2 content, but *t*CA treatment increased it. This result aligns with the findings of Tawfik et al. (2021), who demonstrated that iron oxide nanoparticles reduced hydrogen peroxide contents in *Moringa oleifera* leaves, and the report of Kapoor et al. (2021), who reported increased H_2O_2 levels in *Pisum sativum* plants treated with cinnamic acid. Fe_3O_4-NP treatment has been shown to reduce H_2O_2 accumulation and preserve cell membrane integrity (Jalali et al., 2017). Iron influences the proper functioning of many enzymes, especially at the active sites of catalase and superoxide dismutase, which are involved in the detoxification of reactive oxygen species (Tawfik et al., 2021).

The exogenous application of phenylalanine led to reduced H_2O_2 accumulation in tomato fruits due to increased activity of ROS scavenging enzymes (Soleimani Aghdam et al., 2019). Sanikhani et al. (2020) conducted a study on the effect of phenylalanine on *Citrullus colocynthis*. The application of 500 mg L^{-1} phenylalanine resulted in a significant increase in total phenolic and flavonoid contents, about 2- to 3-fold compared to the control. The applications of two phenolic acids also enhanced the contents of phenolic compounds and flavonoids in rice leaves and roots (Xuan and Khang, 2018). Moreover, Hassan and Jassim (2018) investigated the effects of L-phenylalanine on alkaloid production in *Trigonella foenum-graecum* L., suggesting a potential role of phenylalanine in modulating alkaloid biosynthesis in plant.

Maintaining membrane stability is crucial for plant survival under abiotic stresses. In our experiment, MDA levels remained unchanged with Fe_3O_4-NPs treatment but increased under *t*CA and L-Phe treatments. This observation is consistent with the role of MDA as an
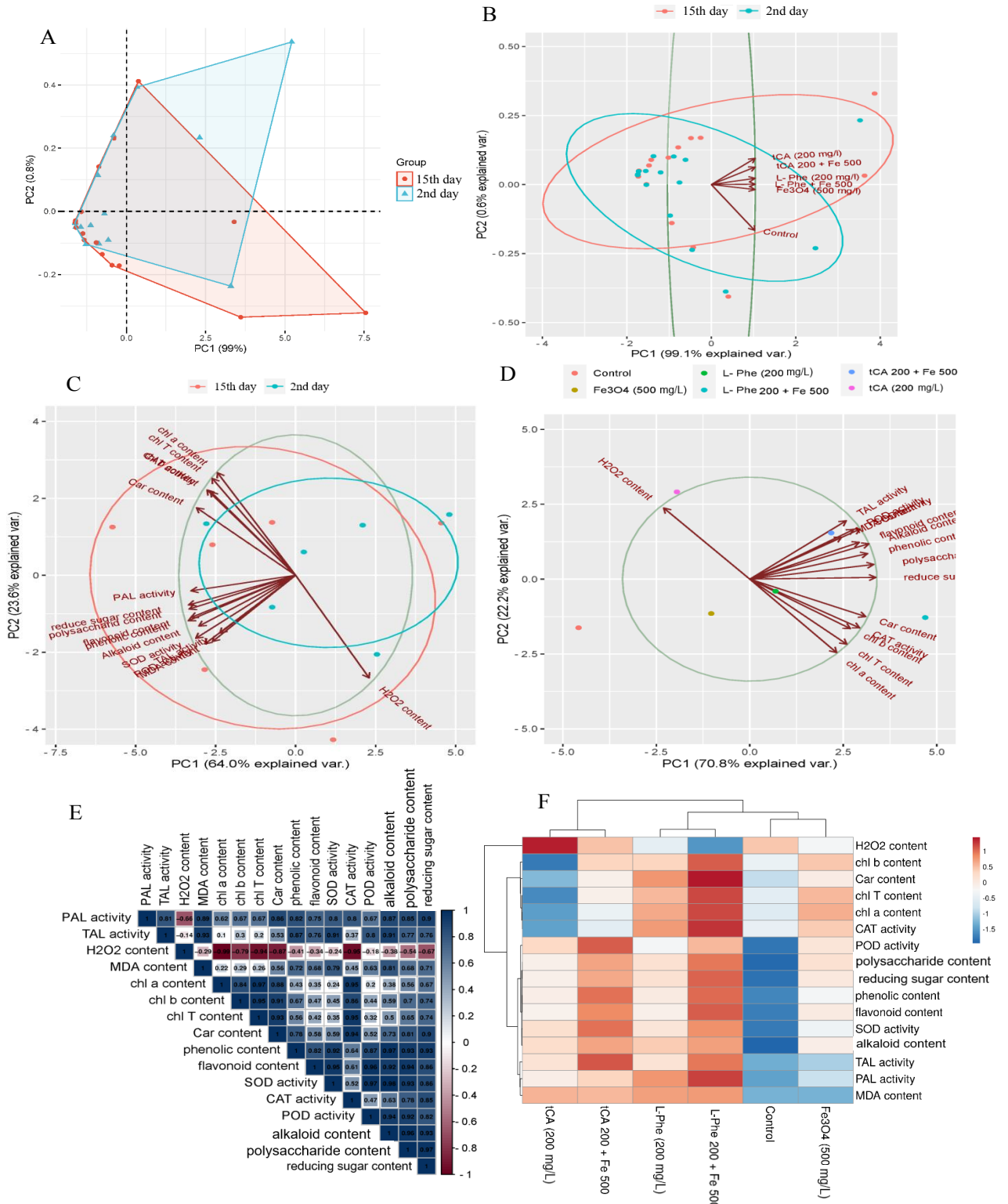
Figure 11. Biplot obtained from principal component analysis (PCA) of the two data sets on the 2nd and 15th days after treatments (A). Correlation between treatments and control at two experiment times (B). Variable correlation plots between all samples show the distance between variables on the 2nd and 15th days after treatments (C) and between different treatments (D). Pearson's correlation matrix between variables, correlations are displayed in blue (positive) and red (negative) and color intensity is proportional to the correlation coefficient (E). Heatmap showing data distribution among five samples treated with elicitors and control in *N. tazetta* plants (F).

indicator of lipid peroxidation and cellular damage under stress conditions (Shah et al., 2020; Koleva et al., 2022). Increased MDA production can enhance plasma membrane permeability, leading to the leakage of cellular contents and subsequent damage to vital processes such as photosynthesis and respiration, ultimately resulting in cell death (Zhang et al., 2021; Janku et al., 2019). Thus, MDA content could be utilized as a valuable diagnostic indicator of stress conditions in plants (Zhang et al., 2021). Interestingly, previous studies have shown contradictory effects on MDA levels in response to different treatments. For instance, MDA levels decreased in wheat plants treated with Fe_3O_4-NPs (Feng et al., 2022), suggesting a protective effect against oxidative stress. Conversely, the increase in MDA content in pea plants treated with cinnamic acid indicates the presence of oxidative stress resulting from the overproduction of ROS (Kapoor et al., 2021).

Treatments of *N. tazetta* with Fe_3O_4-NPs alone or combined with *t*CA or L-Phe led to increased activities of antioxidant enzymes. In response to the potential damage caused by ROS in plants, two antioxidant systems come into play: enzymatic and nonenzymatic antioxidants (Agarwal and Pandey, 2004). Enzymatic antioxidants are particularly important in preventing uncontrolled oxidation cascades within plants. For instance, superoxide dismutase served as the first line of defense, converting superoxide anion into peroxide, while Catalase plays a crucial role in converting H_2O_2 into oxygen and water (Koleva et al., 2022). Iron plays a vital role in redox systems, including its involvement in heme proteins (such as catalase, peroxidase, and cytochromes) and Fe-S proteins (ferredoxin and superoxide dismutase) (Nourozi et al., 2019). Wang et al. (2011) reported increased activities of SOD and CAT in *Lolium perenne* L. and *Cucurbita mixta* plants exposed to Fe_3O_4-NPs, indicating their role in enhancing antioxidant defenses. Similarly, foliar and seed applications of phenylalanine led to increased antioxidant activities (SOD, POD, and CAT) in soybean (Teixeira et al., 2017). These findings highlight the potential of Fe_3O_4-NPs and phenylalanin in enhancing the antioxidant capacity of plant, thereby mitigating oxidative stress and promoting plant health for biosynthesis and accumulation of metabolites.

Our results showed that under *t*CA treatment, SOD and POD activities increased, but CAT activity decreased. Cinnamic acid is known to induce oxidative stress (Ye et al., 2006), which can explain the observed increase in the activity of these antioxidant enzymes. Similar results were reported by other researchers (Singh et al., 2013; Sun et al., 2012; Kapoor et al., 2021), who reported that cinnamic acid enhanced the activities of SOD, APX, and GPX. In *Solanum lycopersicum*, phenolic compounds were found to increase antioxidant activities (Hussain et al., 2017),

further supporting the role of phenolic compounds, such as cinnamic acid, in modulating antioxidant responses in plants.

In our experiment, we focused on PAL and TAL enzymes due to their association with phenylalanine and tyrosine metabolism. PAL, the first regulatory enzyme in the phenylpropanoid metabolism (Kong, 2015), triggers the switch from the plant's primary to the secondary metabolism. PAL activity causes the formation of a wide range of secondary metabolites with a phenylpropanoid skeleton (Rohde et al., 2004). Interestingly, PAL can also utilize tyrosine alongside phenylalanine in metabolic processes (Feduraev et al., 2020). Research by Barros et al. (2016) highlighted that phenolic compounds in *Brachypodium distachyon* originate from tyrosine. In fact, tyrosine is directly converted into *p*-coumaric acid by bifunctional phenylalanine and tyrosine ammonia-lyase (PTAL). These enzymes can be activated under different biotic and abiotic stresses, making them ideal candidates for elicitor-induced signaling reactions (Feduraev et al., 2020). We observed significant increases in PAL and TAL activities under all treatments. L-Phe serves as the precursor of the PAL enzyme and facilitates the progression of the alkaloid biosynthetic pathway, while *t*CA is the first product and Fe is a necessary cofactor for numerous enzymes involved in these pathways. Figure 7 shows that there are significant differences between expressions of the two genes. PAL and N4OMT are the enzymes in the primary and intermediate stages of narcissus alkaloid biosynthesis, respectively. Our finding indicate that the highest activity of PAL and TAL enzymes was observed on the 2nd and 15th days after treatment, particularly with treatment involving L-Phe or *t*CA (200 mg L^{-1}) combined with Fe_3O_4-NPs (500 mg L^{-1}). Conversely, the maximum expression of the N4OMT gene was noted at 24 h after applied treatments. In silico analysis conducted in this study revealed that Fe_3O_4-NPs and *t*CA exhibited greater binding affinity for the N4OMT enzyme, while the L-Phe precursor demonstrated a stronger propensity to bind to PAL compared to N4OMT. Several isoforms of the PAL enzyme coexist in cells, and their products serve as vital substrates for the N4OMT enzyme. Hence, the maximum activity of the latter enzyme occurs 24 h after treatment. As a result of circadian fluctuations, expression of the PAL genes can be increased again at 96 h after treatments. Consequently, after 15 days of treatments, the content of phenolic and alkaloid compounds showed a significant increase compared to the control.

Treatment of *T. aestivum* L. seedling with phenylalanine and tyrosine as exogenous precursors led to significant increase in the expression of PAL6, C3H1, C4H1, and 4CL1 gene. Notably, phenylalanine exhibited a stronger stimulatory effect on most genes compared to tyrosine

(Feduraev et al., 2020). Additionally, Nourozi et al. (2019) investigated the effect of Fe_3O_4-NPs on phenylalanine ammonia-lyase (PAL) and rosmarinic acid synthase (RAS) genes in *Deracocephalum kotschyi*. Their result indicated that expression levels of these genes were influenced by both elicitor concentration and exposure time. For a short time, increasing Fe_3O_4-NPs concentrations after 48 h resulted in a slight enhancement in the expression levels of PAL and RAS genes. These findings align with the results reported by Feduraev et al. (2020), where significant increases in PAL and TAL activities were observed in wheat plants exposed to a medium containing 500 µM phenylalanine and tyrosine for 4 h. Moreover, the use of phenylalanine enhanced the PAL activity in soybean, whether applied as a foliar or seed treatment (Teixeira et al., 2017).

Our research demonstrated that treating plants with Fe_3O_4-NPs alone or combined with L-Phe or *t*CA led to an increase in the photosynthetic pigments including chlorophyll *a*, chlorophyll *b*, total chlorophyll, and carotenoids. Photosynthesis is the most vital source of energy for plant growth, relies heavily on chlorophyll, a crucial pigment for this process (Baker, 2008). Chlorophyll *a* and *b* absorb sunlight at distinct wavelengths, with the total chlorophyll content directly impacting the plant's photosynthetic capacity (Li et al., 2018). Iron plays a role in the synthesis of aminolaevulinic acid and protochlorophyllide (Tawfik et al., 2021). It is necessary for maintaining the structure and function of the chloroplasts. Additionally, Fe is part of electron transport systems (Mai and Bauer, 2016).

Several studies support our findings. For example, Fe_3O_4-NPs treatment enhances chlorophyll content and net photosynthetic rate in *Pseudostellaria heterophylla* (Li et al., 2021). Feng et al. (2022) studied the effects of Fe_3O_4-NPs on wheat plants. Their results revealed that high concentrations of Fe_3O_4-NPs increased plant growth, photosynthetic pigment contents and the activity of rubisco. Also, plants treated with Fe_3O_4-NPs maintained a higher content of potassium and phosphorus which are essential for the activity of the Calvin cycle and dark respiration enzymes. Fe_3O_4-NPs treatment was also shown to stimulate iron oxygen reductase activity, indirectly promoting the metabolism of porphyrin, a chlorophyll precursor (Maswada et al., 2018). Fe_3O_4-NPs increased chlorophyll content in *Quercus macdougallii* (Pariona et al., 2017). Similarly, foliar spray of L-phenylalanine significantly increased chlorophyll content, as well as the fresh and dry weights, under fungi and bacteria inoculation (Rahmani-Samani et al., 2019). This research also revealed that *t*CA treatment decreased the contents of photosynthetic pigments. *t*CA-induced allelochemical stress may interfere with the synthesis of porphyrin, a precursor to chlorophyll (Kapoor et al., 2021). The study

by Baziramakenga et al. (1994) supports our finding, as they reported a reduction in leaf chlorophyll content in soybeans treated with cinnamic acid, similar to the decrease observed with *t*CA treatment in our study.

Phosphoproteomic analyses of thylakoid membrane proteome in Fe-sufficient and Fe-deficient plants revealed post-translational modifications in some proteins such as PSBH, ascorbate peroxidase, peroxiredoxin Q, and two major LHC IIb proteins (Laganowsky et al., 2009). Thus, it can be concluded that Fe_3O_4-NPs application, along with precursors, affects the photosynthetic system and increases photosynthetic pigments and carbohydrate contents. According to De Ridder and Salvucci's results (2007), it seems that the greater sensitivity of photosystem II, increasing photosynthesis efficiency and O_2 evolution, and 3-phosphoglycerate accumulation all play a role in increasing the content of proline and soluble sugar under fertilizer application. These findings and our results contribute to deeper understanding of the intricate interplay between Fe_3O_4-NPs and exogenous precursors in modulating plant photosynthesis and pigment metabolism.

In plant cells, soluble sugars are vital for osmotic adjustment and protecting the structure of macromolecules and cell membranes (Tawfik et al., 2021). In our research, along with the increase in photosynthetic pigments, the content of soluble sugars and polysaccharides increased after all treatment groups. The effects of Fe and amino acids like phenylalanine on increasing polysaccharide and soluble sugar contents might be due to their role in chlorophyll biosynthesis, which influences carbohydrate metabolism (Wahba et al., 2015). Couée et al. (2006) highlighted the dual role of sugars in regulating ROS, suggesting that soluble sugars can both contribute to ROS production and serve as substrates for processes generating NADPH, such as the oxidative pentose-phosphate pathway (OPPP), thereby aiding in ROS scavenging. The increased NADPH/$NADP^+$ ratio and synthesis of some intermediates due to enhanced OPPP activity can provide precursors required for the production of phenolic and alkaloid metabolites. Hence, there seems to be a logical association between the increase in production of phenolic and flavonoid compounds of narcissus leaf and the treatment of Fe_3O_4-NPs and precursors especially L-Phe in this research.

Our findings are supported by previous studies. For instance, El-Nasr (2015) demonstrated that foliar spray with magnetite (Fe_3O_4) nanoparticles increased total carbohydrate contents in pear saplings (*Pyrus serotina* L. × *Pyrus communis* L.). Talaat and Balbaa (2010) also observed a significant increase in total carbohydrate and total soluble sugar in sweet basil plants following a foliar spray of *trans*-cinnamic acid. Furthermore, phenylalanine, acting as a nitrogen source, increased starch content in the roots and leaves of poplar trees (Jiao et al., 2018). Terry and

Low (1982) reported a correlation between chlorophyll content and iron accumulation in plant leaves, suggesting that iron treatment may influence the formation and development of new layered thylakoids in chloroplast, which are essential for chlorophyll synthesis.

5. Conclusion

Our study delved into the effects of Fe_3O_4-NPs and precursors of L-Phenyalanine and *trans*-cinnamic acid on Amaryllidaceae alkaloids production in *N. tazetta*. Foliar application of these compounds exhibited significant potential in enhancing alkaloid production. Fe_3O_4-NPs and the precursors induced oxidative stress by signaling H_2O_2 and increasing MDA levels. These changes were accompanied by an increase in the level of phenolic compounds, flavonoids, photosynthetic pigments, and the activity of antioxidant enzymes, which ultimately led to a heightened increase in secondary metabolites including alkaloids (a 1.92-fold increase with Fe_3O_4-NPs and approximately 2.3-fold with combined treatments compared to the control on the 15th day). Moreover, our study revealed an upregulation of PAL and TAL activities, as well as an increase in the expression of the *PAL* and *N4OMT* genes, indicating enhanced progression of the alkaloid biosynthetic pathway. The in silico component of our study provided valuable insights into the molecular interactions between elicitors and biosynthetic enzymes. By elucidating the binding affinities and interactions of elicitors with specific enzyme active sites, these findings provide a deeper understanding of how elicitors modulate gene expression and enzyme activity. This information is crucial for understanding the signaling pathways involved in plant responses to elicitors and unraveling the regulatory networks governing gene-elicitor interactions. Ultimately, these insights contribute to the broader understanding of plant defense mechanisms, regulate metabolic pathways, and facilitate the development of scientific strategies to increase plant productivity under different conditions.

Conflicts of interest
The authors declare no conflicts of interest

References

Abdelkawy AM, Alshammari SO, Hussein HA, Abou El-Enain IMM, Abdelkhalek ES et al. (2023). Effect of silver nanoparticles on tropane alkaloid production of transgenic hairy root cultures of *Hyoscyamus muticus* L. and their antimicrobial activity. Scientific Reports 13 (1): 1-9. https://doi.org/10.1038/s41598-023-36198-x

Abdelsattar AS, Dawoud A, Helal MA (2021) Interaction of nanoparticles with biological macromolecules: a review of molecular docking studies. Nanotoxicology 15 (1): 66-95. https://doi.org/10.1080/17435390.2020.1842537

Agarwal S, Pandey V (2004). Antioxidant enzyme responses to NaCl stress in *Cassia angustifolia*. Biologia Plantarum 48 (4): 555-560. https://doi.org/10.1023/B:BIOP.0000047152.07878.e7

Alkhatib R, Abdo N, Al-Eitan L, Kafesha R, Rousan A (2020). Impact of magnetically treated water on the growth and development of tobacco (*Nicotiana tabacum* var. Turkish). Physiology and Molecular Biology of Plants: An International Journal of Functional Plant Biology 26 (5): 1047-1054. https://doi.org/10.1007/s12298-020-00787-1

Avellan A, Yun J, Zhang Y, Spielman-Sun E, Unrine JM et al. (2019). Nanoparticle size and coating chemistry control foliar uptake pathways, translocation, and leaf-to-rhizosphere transport in wheat. ACS Nano 13: 5291–5305. https://doi.org/10.1021/acsnano.8b09781

Baker NR (2008). Chlorophyll fluorescence: a probe of photosynthesis in vivo. Annual Review of Plant Biology 59: 89–113. https://doi.org/10.1146/annurev.arplant.59.032607.092759

Barros J, Serrani-Yarce JC, Chen F, Baxter D, Venables BJ et al. (2016). Role of bifunctional ammonia-lyase in grass cell wall biosynthesis. Nature Plants 2: 16050. https://doi.org/10.1038/nplants.2016.50

Bastida Armengol J, Berkov S, Torras Clavería L, Pigni NB, Andradre JPD et al. (2011). Chemical and biological aspects of Amaryllidaceae alkaloids. In: Munoz-Torrero D (editor). Recent advances in Pharmaceutical Sciences, Chapter 3: 65-100.

Baziramakenga R, Simard RR, Leroux GD (1994). Effect of benzoic and cinnamic acids on growth, mineral composition, and chlorophyll contents of soybean. Journal of Chemical Ecology 20: 2821–2833. https://doi.org/10.1007/BF02098391

Beauchamp C, Fridovich I (1971). Superoxide dismutase: Improved assays and an assay applicable to acrylamide gels. Analytical Biochemistry 44 (1): 276-287. https://doi.org/10.1016/0003-2697(71)90370-8

Bradford MM (1976). A rapid and sensitive method for the quantitation of microgram quantities of protein utilizing the principle of protein-dye binding. Analytical Biochemistry 72 (1-2): 248-254. https://doi.org/10.1016/0003-2697(76)90527-3

Chen C, Wu J, Hua Q, Tel-Zur N, Xie F et al. (2019). Identification of reliable reference genes for quantitative real-time PCR normalization in pitaya. Plant Methods 15: 70. https://doi.org/10.1186/s13007-019-0455-3

Couée I, Sulmon C, Gouesbet G, El Amrani A (2006). Involvement of soluble sugars in reactive oxygen species balance and responses to oxidative stress in plants. Journal of Experimental Botany 57(3): 449-459. https://doi.org/10.1093/jxb/erj027

Dazy M, Béraud E, Cotelle S, Meux E, Masfaraud JF et al. (2008). Antioxidant enzyme activities as affected by trivalent and hexavalent chromium species in *Fontinalis antipyretica* Hedw. Chemosphere 73: 281-290. https://doi.org/10.1016/j.chemosphere.2008.06.044

De Ridder BP, Salvucci ME (2007). Modulation of rubisco activase gene expression during heat stress in cotton (*Gossypium hirsutum* L.) involves post-transcriptional mechanisms. Plant Science 172 (2):246–254. https://doi.org/10.1016/j.plantsci.2006.08.014

Desgagné-Penix I (2020). Biosynthesis of alkaloids in Amaryllidaceae plants: a review. Phytochemistry Reviews 20 (2): 409-431. https://doi.org/10.1007/s11101-020-09678-5

Dubois M, Gilles KA, Hamilton JK, Rebers PT, Smith F (1956). Colorimetric method for determination of sugars and related substances. Analytical Chemistry 28 (3): 350–356. https://doi.org/10.1021/ac60111a017

Elekes CC, Dumitriu I, Busuioc G, Iliescu NS (2010). The appreciation of mineral element accumulation level in some herbaceous plant species by ICP–AES method. Environmental Science and Pollution Research 17:1230–1236. https://doi.org/10.1007/s11356-010-0299-x

El-Nasr A, El-Hennawy HM, El-Kereamy AMH, Abou El-Yazied A, Salah Eldin TA (2015). Effect of magnetite nanoparticles (Fe$_3$O$_4$) as nutritive supplement on pear saplings. Middle East Journal of Applied Science 5(3): 777–785.

Evidente A (2023). Advances on the Amaryllidacea alkaloids collected in south Africa, Andean south America and the mediterranean basin. Molecules 28 (10): 4055. https://doi.org/10.3390/molecules28104055

Feduraev P, Skrypnik L, Riabova A, Pungin A, Tokupova E et al. (2020). Phenylalanine and tyrosine as exogenous precursors of wheat (*Triticum aestivum* L.) secondary metabolism through PAL-associated pathways. Plants 9 (4): 476. https://doi.org/10.3390/plants9040476

Feng K, Liu JX, Xing GM, Sun S, Li S et al. (2019). Selection of appropriate reference genes for RT-qPCR analysis under abiotic stress and hormone treatment in celery. PeerJ 7: e7925. https://doi.org/10.7717/peerj.7925

Feng Y, Kreslavski VD, Shmarev AN, Ivanov AA, Zharmukhamedov SK et al. (2022). Effects of iron oxide nanoparticles (Fe$_3$O$_4$) on growth, photosynthesis, antioxidant activity and distribution of mineral elements in wheat (*Triticum aestivum*) plants. Plants 11 (14): 1894. https://doi.org/10.3390/plants11141894

Gandhi S, Roy I (2019). Synthesis and characterization of manganese ferrite nanoparticles, and its interaction with bovine serum albumin: a spectroscopic and molecular docking approach. Journal of Molecular Liquids 296: 111871. https://doi.org/10.1016/j.molliq.2019.111871

Ghazanfari MR, Kashefi M, Shams SF, Jaafari MR (2016). Perspective of Fe$_3$O$_4$ nanoparticle role in biomedical applications. Biochemistry Research International 2016: 1-32. https://doi.org/10.1155/2016/7840161

Hadizadeh M, Hamideh O, Kianirad M, Amidi Z (2019). Elicitation of pharmaceutical alkaloids biosynthesis by salicylic acid in marine microalgae *Arthrospira platensis*. Algal Research, 42: 101597. https://doi.org/10.1016/j.algal.2019.101597

Halder M, Sarkar S, Jha S. (2019). Elicitation: a biotechnological tool for enhanced production of secondary metabolites in hairy root cultures. Engineering in Life Science 19 (12): 880-895. https://doi.org/10.1002/elsc.201900058

Hanks GR (2002). Narcissus and daffodil-the genus *Narcissus*. In: Hardman R (editor). Medicinal and aromatic plants-industrial profiles. Taylor & Francois, London, 21. https://doi.org/10.1201/9780203219355

Harsini MG, Habibi H, Talaei GH (2014). Study the effects of iron nano chelated fertilizers foliar application on yield and yield components of new line of wheat cold region of kermanshah province. Agricultural Advances 3 (4): 95-102. https://civilica.com/doc/500693

Hassan SA, Jassim EH (2018). Effect of L-phenylalanine on the production of some alkaloids and steroidal saponins of fenugreek cotyledons derived callus. Pakistan Journal of Biotechnology 15 (2): 481-486. https://pjbt.org/index.php/pjbt/article/view/420

Heath RL, Packer L (1968). Photoperoxidation in isolated chloroplasts. I. Kinetics and stoichiometry of fatty acid peroxidation. Archives in Biochemistry and Biophysics 125: 189–198. https://doi.org/10.1016/0003-9861(68)90654-1

Hotchandani T, de Villers J, Desgagné-Penix I (2019). Developmental regulation of the expression of Amaryllidaceae alkaloid biosynthetic genes in *Narcissus papyraceus*. Genes 10 (8): 595. https://doi.org/10.3390/genes10080594

Howlett BJ (2006). Secondary metabolite toxins and nutrition of plant pathogenic fungi. Current Opinion in Plant Biology 9 (4): 371-375. https://doi.org/10.1016/j.pbi.2006.05.004

Hu J, Guo H, Li J, Gan Q, Wang Y et al. (2017). Comparative impacts of iron oxide nanoparticles and ferric ions on the growth of *Citrus maxima*. Environment Pollution 221: 199–208. https://doi.org/10.1016/j.envpol.2016.11.064

Hulcová D, Maříková J, Korábečný J, Hošťálková A, Jun D et al. (2019). Amaryllidaceae alkaloids from *Narcissus pseudonarcissus* L. cv. Dutch Master as potential drugs in treatment of Alzheimer's disease. Phytochemistry 165: 112055. https://doi.org/10.1016/j.phytochem.2019.112055

Hussain I, Singh NB, Singh A, Singh H, Singh SC et al. (2017). Exogenous application of photosynthesized nanoceria to alleviate ferulic acid stress in *Solanum lycopersicum*. Scientia Horticulturae 214: 158-164. https://doi.org/10.1016/j.scienta.2016.11.032

Hussain MS, Fareed S, Ansari S, Rahman MA, Ahmad IZ et al. (2012). Current approaches toward production of secondary plant metabolites. Journal of Pharmacy and Bioallied Sciences 4 (1): 10-20. https://doi.org/10.4103/0975-7406.92725

Jalali M, Ghanati F, Modarres-Sanavi AM, Khoshgoftarmanesh AH (2017). Physiological effects of repeated foliar application of magnetite nanoparticles on maize plants. Journal of Agronomy and Crop Science 203: 593–602. https://doi.org/10.1111/jac.12208

Janku ML, Luhov Á, Petrivalský M (2019). On the origin and fate of reactive oxygen species in plant cell compartments. Antioxidants 8:105. https://doi.org/10.3390/antiox8040105

Jiao Y, Chen Y, Ma C, Qin J, Nguyen THN et al. (2018). Phenylalanine as a nitrogen source induces root growth and nitrogen-use efficiency in *Populus × canescens*. Tree Physiology 38 (1): 66–82. https://doi.org/10.1093/treephys/tpx109

Joshi CJ, Ke W, Drangowska-Way A, O'Rourke EJ, Lewis NE (2022). What are housekeeping genes? PLOS Computational Biology 18 (7): e1010295. https://doi.org/10.1371/journal.pcbi.1010295

Kafayati ME, Raheb J, Torabi Angazi M, Alizadeh S et al. (2013). The effect of magnetic Fe_3O_4 nanoparticles on the growth of genetically manipulated bacterium, *Pseudomonas aeruginosa* (PTSOX4). Iranian Journal of Biotechnology 11 (1): 41-46. https://doi.org/10.5812/IJB.9302

Kapoor RT, Alyemeni MN, Ahmad P (2021). Exogenously applied spermidine confers protection against cinnamic acid-mediated oxidative stress in *Pisum sativum*. Saudi Journal of Biological Sciences 28 (5): 2619-2625. https://doi.org/10.1016/j.sjbs.2021.02.052

Khalil AT, Ayaz M, Ovais M, Wadood A, Ali M et al. (2018). In vitro cholinesterase enzymes inhibitory potential and *in Silico* molecular docking studies of biogenic metal oxides nanoparticles. Inorganic and Nano-Metal Chemistry 48: 441–448. https://doi.org/10.1080/24701556.2019.1569686

Klosi R, Mersinllari M, Gavani E (2016). Galantamine content in *Leucojum aestivum* populations grown in northwest Albania. Albanian Journal of Pharmaceutical Sciences 3, 3-5.

Koleva L, Umar A, Yasin NA, Shah AA, Siddiqui MH et al. (2022). Iron oxide and silicon nanoparticles modulate mineral nutrient homeostasis and metabolism in cadmium-stressed *Phaseolus vulgaris*. Frontiers in Plant Science 13: 806781. https://doi.org/10.3389/fpls.2022.806781

Kołton A, Długosz-Grochowska O, Wojciechowska R, Czaja M (2022). Biosynthesis regulation of folates and phenols in plants. Scientia Horticulturae 291: 110561. https://doi.org/10.1016/j.scienta.2021.110561

Kong JQ (2015) Phenylalanine ammonia-lyase, a key component used for phenylpropanoids production by metabolic engineering. RSC Advances 5: 62587–62603. https://doi.org/10.1039/C5RA08196C

Kyndt JA, Meyer TE, Cusanovich MA, Van Beeumen JJ (2002). Characterization of a bacterial tyrosine ammonia lyase, a biosynthetic enzyme for the photoactive yellow protein. FEBS Letters 512(1-3): 240-244. https://doi.org/10.1016/S0014-5793(02)02272-X

Laganowsky A, Gómez SM, Whitelegge JP, Nishio JN (2009). Hydroponics on a chip: analysis of the Fe deficient *Arabidopsis* thylakoid membrane proteome. Journal of Proteomics 72(3): 397-415. https://doi.org/10.1016/j.jprot.2009.01.024

Li J, Hu J, Xiao L, Wang Y, Wang X (2018). Interaction mechanisms between α- Fe_2O_3, γ-Fe_2O_3 and Fe_3O_4 nanoparticles and *Citrus maxima* seedlings. Science of Total Environment 625: 677–685. https://doi.org/10.1016/j.scitotenv.2017.12.276

Li J, Ma Y, Xie Y (2021). Stimulatory effect of Fe_3O_4 nanoparticles on the growth and yield of *Pseudostellaria heterophylla* via improved photosynthetic performance. HortScience 56 (7): 753–761. https://doi.org/10.21273/HORTSCI15658-20

Li W, Qiao C, Pang J, Zhang G, Luo Y (2019). The versatile O-methyltransferase L4OMT catalyzes multiple O-methylation reactions in Amaryllidaceae alkaloids biosynthesis. International Journal of Biological Macromolecules141: 680–692. https://doi.org/10.1016/j.ijbiomac.2019.09.011

Li Y, He N, Hou J, Xu L, Liu C et al. (2018). Factors influencing leaf chlorophyll content in natural forests at the biome scale. Frontiers in Ecology and Evolution 6: 324791. https://doi.org/10.3389/fevo.2018.00064

Lichtenthaler HK (1987). Chlorophylls and carotenoids: Pigments of photosynthetic biomembranes. Methods in Enzymology 148: 350-382. https://doi.org/10.1016/0076-6879(87)48036-1

Liu D, Wen J, Liu J, Li L (1999). The roles of free radicals in amyotrophic lateral sclerosis: Reactive oxygen species and elevated oxidation of protein, DNA, and membrane phospholipids. The FASEB Journal 13 (15): 2318–2328. https://doi.org/10.1096/fasebj.13.15.2318

Livak KJ, Schmittgen TD (2001). Analysis of relative gene expression data using real-time quantitative PCR and the $2^{-\Delta\Delta C_T}$ method. Methods 25 (4): 402–408. https://doi.org/10.1006/meth.2001.1262

Lv J, Christie P, Zhang S (2019). Uptake, translocation, and transformation of metal-based nanoparticles in plants: Recent advances and methodological challenges. Environmental Science: Nano 6: 41–59. https://doi.org/10.1039/C8EN00645H

Mai HJ, Bauer P (2016). From the proteomic point of view: integration of adaptive changes to iron deficiency in plants. Current Plant Biology 5: 45–56. https://doi.org/10.1016/j.cpb.2016.02.001

Maswada HF, Djanaguiraman M, Prasad PVV (2018). Seed treatment with nano-iron (III) oxide enhances germination, seeding growth and salinity tolerance of sorghum. Journal of Agronomy and Crop Science 204 (6): 577– 587. https://doi.org/10.1111/jac.12280

Moe LA (2013). Amino acids in the rhizosphere: from plants to microbes. American Journal of Botany 100 (9): 1692–1705. https://doi.org/10.3732/ajb.1300033

Nourozi E, Hosseini B, Maleki R, Abdollahi Mandoulakani B (2019). Iron oxide nanoparticles: a novel elicitor to enhance anticancer flavonoid production and gene expression in *Dracocephalum kotschyi* hairy-root cultures. Journal of the Science of Food and Agriculture 99 (14): 6418-6430. https://doi.org/10.1002/jsfa.9921

Pandey V, Patel A, Patra DD (2015). Amelioration of mineral nutrition productivity, antioxidant activity and aroma profile in marigold (*Tagetes minuta* L.) with organic and chemical fertilization. Industrial Crops and Products 76: 378–385. https://doi.org/10.1016/j.indcrop.2015.07.023

Pariona N, Martinez AI, Hernandez-Flores H, Clark-Tapia R (2017). Effect of magnetite nanoparticles on the germination and early growth of *Quercus macdougallii*. Science of the Total Environment 575: 869–875. https://doi.org/10.1016/j.scitotenv.2016.09.128

Rahmani-Samani M, Ghasemi Pirbalouti A, Moattar F, Golparvar AR (2019). L-Phenylalanine and bio-fertilizers interaction effects on growth, yield and chemical compositions and content of essential oil from the sage (*Salvia officinalis* L.) leaves. Industrial Crops and Products 137: 1-8. https://doi.org/10.1016/j.indcrop.2019.05.019

Ramachandra CT, Srinivasa Rao PS (2008). Processing of *Aloe vera* leaf gel: a review. American Journal of Agricultural and Biological Sciences 3 (2): 502-551. https://doi.org/10.3844/ajabssp.2008.502.510

Renaudin JP (1984). Reversed-phase HPLC characteristics of indole alkaloids from cell suspension cultures of *Catharanthus roseus* L. Chromatography 291:165-174.

Rivero-Montejo SDJ, Vargas-Hernandez M, Torres-Pacheco I (2021). Nanoparticles as novel elicitors to improve bioactive compounds in plants. Agriculture 11 (2): 134. https://doi.org/10.3390/agriculture11020134

Rohde A, Morreel K, Ralph J, Goeminne G, Hostyn V et al. (2004). Molecular phenotyping of the *pal1* and *pal2* mutants of *Arabidopsis thaliana* reveals far-reaching consequences on phenylpropanoid, amino acid, and carbohydrate metabolism. Plant Cell 16: 2749–2771. https://doi.org/10.1105/tpc.104.023705

Sanikhani M, Akbari A, Kheiry A (2020). Effect of phenylalanine and tryptophan on morphological and physiological characteristics in colocynth (*Citrullus colocynthis* L.). Journal of Plant Process and Function 9 (35): 317-328.

Shah AA, Khan WU, Yasin NA, Akram W, Ahmad A et al. (2020). Butanolide alleviated cadmium stress by improving plant growth, photosynthetic parameters and antioxidant defense system of *Brassica oleracea*. Chemosphere 261:127728. https://doi.org/10.1016/j.chemosphere.2020.127728

Singh PK, Singh R, Sing S (2013). Cinnamic acid induced changes in reactive oxygen species scavenging enzymes and protein profile in maize (*Zea mays* L.) plants grown under salt stress. Physiology and Molecular Biology of Plants 19 (1): 53-59. https://doi.org/10.1007/s12298-012-0126-6

Smirnoff N, Arnaud D (2019). Hydrogen peroxide metabolism and functions in plants. New Phytologist 221 (3): 1197-1214. https://doi.org/10.1111/nph.15488

Soleimani Aghdam M, Moradi M, Razavi F, Rabiei V (2019). Exogenous phenylalanine application promotes chilling tolerance in tomato fruits during cold storage by ensuring supply of NADPH for activation of ROS scavenging systems. Scientia Horticulturae 246: 818–825. https://doi.org/10.1016/j.scienta.2018.11.074

Somogyi M (1952). Notes on sugar determination. Journal of Biological Chemistry 195: 19–23.

Sun WJ, Nie YX, Gao Y, Dai AH, Bai JG (2012). Exogenous cinnamic acid regulates antioxidant enzyme activity and reduces lipid peroxidation in drought-stressed cucumber leaves. Acta Physiologiae Plantarum 34: 641–655. https://doi.org/10.1007/s11738-011-0865-y

Swanson BG (2003). Tannins and polyphenols. In: Caballero B, Trugo L, Finglas P (editors). Encyclopedia of Food Sciences and Nutrition, 2nd ed. Academic Press, 5729-5733. https://doi.org/10.1016/B0-12-227055-X/01178-0

Talaat IM, Balbaa LK (2010). Physiological response of sweet basil plants (*Ocimum basilicum* L.) to putrescine and *trans*-cinnamic acid. American-Eurasian Journal of Agricultural and Environmental Science 8 (4): 438-445. https://api.semanticscholar.org/CorpusID:102300425

Tawfik MM, Mohamed MH, Sadak MS, Thalooth AT (2021). Iron oxide nanoparticles effect on growth, physiological traits and nutritional contents of *Moringa oleifera* grown in saline environment. Bulletin of the National Research Centre 45 (1): 177, 1-9. https://doi.org/10.1186/s42269-021-00624-9

Teixeira WF, Fagan EB, Soares LH, Umburanas RC, Reichardt K et al. (2017). Foliar and seed application of amino acids affects the antioxidant metabolism of the soybean crop. Frontiers in Plant Science 8: 327. https://doi.org/10.3389/fpls.2017.00327

Terry N, Low G (1982). Leaf chlorophyll content and its relation to the intracellular localization of iron. Journal of Plant Nutrition 5 (4-7): 301-310. https://doi.org/10.1080/01904168209362959

Tunc-Ozdemir M, Miller G, Song L, Kim J, Sodek A et al. (2009). Thiamin confers enhanced tolerance to oxidative stress in Arabidopsis. Plant Physiology 151 (1): 421-432. https://doi.org/10.1104/pp.109.140046

Van Goietsenoven G, Hutton J, Becker JP, Lallemand B, Robert F et al. (2010). Targeting of eEF1A with Amaryllidaceae isocarbostyrils as a strategy to combat melanomas. The FASEB Journal 24 (11): 4575–84. https://doi.org/10.1096/fj.10-162263

Vance ME, Kuiken T, Vejerano EP, McGinnis SP, Hochella Jr MF et al. (2015). Nanotechnology in the real world: redeveloping the nanomaterial consumer products inventory. Beilstein Journal of Nanotechnology 6: 1769-1780. https://doi.org/10.3762/bjnano.6.181

Velikova V, Yordanov I, Edreva AJPS (2000). Oxidative stress and some antioxidant systems in acid rain-treated bean plants. Protective role of exogenous polyamines. Plant Science 151 (1): 59–66. https://doi.org/10.1016/S0168-9452(99)00197-1

Wahba HE, Motawe HM, Ibrahim AY (2015). Growth and chemical composition of *Urtica pilulifera* L. plant as influenced by foliar application of some amino acids. Journal of Materials and Environmental Science 6 (2): 499-509.

Wang H, Kou X, Pei Z, Xiao JQ, Shan X et al. (2011). Physiological effects of magnetite (Fe_3O_4) nanoparticles on perennial ryegrass (*Lolium perenne* L.) and pumpkin (*Cucurbita mixta*) plants. Nanotoxicology 5 (1): 30–42. https://doi.org/10.3109/17435390.2010.489206.

Wang X, Xie H, Wang P, Yin H (2023). Nanoparticles in plants: uptake, transport and physiological activity in leaf and root. Materials (Basel) 16 (8): 3097. https://doi.org/10.3390/ma16083097

Xuan TD, Khang DT (2018). Effects of exogenous application of protocatechuic acid and vanillic acid to chlorophylls, phenolics and antioxidant enzymes of rice (*Oryza sativa* L.) in submergence. Molecules 23 (3): 620. https://doi.org/10.3390/molecules23030620

Ye SF, Zhou YH, Sun Y, Zou LY, Yu JQ (2006). Cinnamic acid causes oxidative stress in cucumber roots, and promotes incidence of *Fusarium wilt*. Environmental and Experimental Botany 56 (3): 255–262. https://doi.org/10.1016/j.envexpbot.2005.02.010

Zhang B, Zheng LP, Wang JW (2012). Nitric oxide elicitation for secondary metabolite production in cultured plant cells. Applied Microbiology and Biotechnology 93: 455–466. https://doi.org/10.1007/s00253-011-3658-8

Zhang X, Liu CJ (2015). Multifaceted regulations of gateway enzyme phenylalanine ammonia-lyase in the biosynthesis of phenylpropanoids. Molecular Plant 8 (1): 17–27. https://doi.org/10.1016/j.molp.2014.11.001

Zhang Y, Luan Q, Jiang J, Li Y (2021). Prediction and utilization of malondialdehyde in exotic pine under drought stress using near-infrared spectroscopy. Frontiers in Plant Science 12: 735275. https://doi.org/10.3389/fpls.2021.735275

Zhdanov VP (2019). Formation of a protein corona around nanoparticles. Current Opinion in Colloid and Interface Science 41: 95–103. https://doi.org/10.1016/j.cocis.2018.12.002

Zhishen J, Mengcheng T, Jianming W (1999). The determination of flavonoid contents in mulberry and their scavenging effects on superoxide radicals. Food Chemistry 64 (4): 555-559. https://doi.org/10.1016/S0308-8146(98)00102-2